



HAL
open science

Quantum diffusion during inflation and primordial black holes

Chris Pattison, Vincent Vennin, Hooshyar Assadullahi, David Wands

► **To cite this version:**

Chris Pattison, Vincent Vennin, Hooshyar Assadullahi, David Wands. Quantum diffusion during inflation and primordial black holes. *Journal of Cosmology and Astroparticle Physics*, 2017, 10, pp.046. 10.1088/1475-7516/2017/10/046 . hal-01645600

HAL Id: hal-01645600

<https://hal.science/hal-01645600v1>

Submitted on 9 Oct 2024

HAL is a multi-disciplinary open access archive for the deposit and dissemination of scientific research documents, whether they are published or not. The documents may come from teaching and research institutions in France or abroad, or from public or private research centers.

L'archive ouverte pluridisciplinaire **HAL**, est destinée au dépôt et à la diffusion de documents scientifiques de niveau recherche, publiés ou non, émanant des établissements d'enseignement et de recherche français ou étrangers, des laboratoires publics ou privés.

Quantum diffusion during inflation and primordial black holes

Chris Pattison,^a Vincent Vennin,^{b,a} Hooshyar Assadullahi,^{a,c} and David Wands^a

^aInstitute of Cosmology & Gravitation, University of Portsmouth, Dennis Sciamia Building, Burnaby Road, Portsmouth, PO1 3FX, United Kingdom

^bLaboratoire Astroparticule et Cosmologie, Université Denis Diderot Paris 7, 75013 Paris, France

^cSchool of Earth and Environmental Sciences, University of Portsmouth, Burnaby Building, Burnaby Road, Portsmouth, PO1 3QL, United Kingdom

E-mail: hooshyar.assadullahi@port.ac.uk, christopher.pattison@port.ac.uk, vincent.vennin@port.ac.uk, david.wands@port.ac.uk

Abstract. We calculate the full probability density function (PDF) of inflationary curvature perturbations, even in the presence of large quantum backreaction. Making use of the stochastic- δN formalism, two complementary methods are developed, one based on solving an ordinary differential equation for the characteristic function of the PDF, and the other based on solving a heat equation for the PDF directly. In the classical limit where quantum diffusion is small, we develop an expansion scheme that not only recovers the standard Gaussian PDF at leading order, but also allows us to calculate the first non-Gaussian corrections to the usual result. In the opposite limit where quantum diffusion is large, we find that the PDF is given by an elliptic theta function, which is fully characterised by the ratio between the squared width and height (in Planck mass units) of the region where stochastic effects dominate. We then apply these results to the calculation of the mass fraction of primordial black holes from inflation, and show that no more than ~ 1 e -fold can be spent in regions of the potential dominated by quantum diffusion. We explain how this requirement constrains inflationary potentials with two examples.

Keywords: physics of the early universe, inflation, primordial black holes

ArXiv ePrint: [1707.00537](https://arxiv.org/abs/1707.00537)

Contents

1	Introduction and motivations	1
2	Probability distribution of curvature perturbations	4
2.1	The stochastic- δN formalism	4
2.2	Statistical moments of first passage times	7
2.3	The characteristic function approach	7
2.4	The heat equation approach	9
3	Expansion about the classical limit	11
3.1	The characteristic function approach	11
3.2	The heat equation approach	15
4	The stochastic limit	15
4.1	The characteristic function approach	16
4.2	The heat equation approach	18
5	Primordial black holes	21
5.1	Classical limit	21
5.2	Stochastic limit	22
5.3	Recipe for analysing a generic potential	24
5.4	Example 1: $V \propto 1 + \phi^p$	25
5.5	Example 2: running-mass inflation	28
6	Conclusion	30
A	Elliptic theta functions	31
B	Detailed analysis of the model $V \propto 1 + \phi^p$	33

1 Introduction and motivations

Cosmological inflation [1–6] is a period of accelerated expansion that occurred at very high energy in the early Universe. During this epoch, vacuum quantum fluctuations were amplified to become large-scale cosmological perturbations that seeded the cosmic microwave background (CMB) anisotropies and the large-scale structure of our Universe [7–12].

In the range of scales accessible to CMB experiments [13, 14], these perturbations are constrained to be small, at the level $\zeta \simeq 10^{-5}$ until they re-enter the Hubble radius during the radiation era, where ζ is the scalar curvature perturbation. At smaller scales however, they may be sufficiently large so that when they re-enter the Hubble radius, they overcome the pressure forces and collapse to form primordial black holes (PBHs) [15–17].

In practice, PBHs form when the mean curvature perturbation in a given Hubble patch exceeds a threshold denoted $\zeta_c \simeq 1$ [18, 19] (see Ref. [20] for an alternative criterion based on the density contrast rather than the curvature perturbation).

The abundance of PBHs is usually stated in terms of the mass fraction of the Universe contained within PBHs at the time of formation, β . If the coarse-grained curvature perturbation ζ_{cg} follows the probability distribution function (PDF) $P(\zeta_{\text{cg}})$, β is given by [21]

$$\beta(M) = 2 \int_{\zeta_c}^{\infty} P(\zeta_{\text{cg}}) d\zeta_{\text{cg}}. \quad (1.1)$$

Here, ζ_{cg} is obtained from keeping the wavelengths smaller than the Hubble radius at the time of formation,

$$\zeta_{\text{cg}}(\mathbf{x}) = (2\pi)^{-3/2} \int_{k > aH_{\text{form}}} d\mathbf{k} \zeta_{\mathbf{k}} e^{i\mathbf{k}\cdot\mathbf{x}}, \quad (1.2)$$

where a is the scale factor, $H \equiv \dot{a}/a$ is the Hubble scale, and a dot denotes differentiation with respect to cosmic time. In Eq. (1.1), M is the mass contained in a Hubble patch at the time of formation [22–24], $M = 3M_{\text{Pl}}^2/H_{\text{form}}$, where M_{Pl} is the reduced Planck mass.

Observational constraints on β depend on the masses PBHs have when they form. For masses between 10^9g and 10^{16}g , the constraints mostly come from the effects of PBH evaporation on big bang nucleosynthesis and the extragalactic photon background, and typically range from $\beta < 10^{-24}$ to $\beta < 10^{-17}$. Heavier PBHs, with mass between 10^{16}g and 10^{50}g , have not evaporated yet and can only be constrained by their gravitational and astrophysical effects, at the level $\beta < 10^{-11}$ to $\beta < 10^{-5}$ (see Refs. [25, 26] for summaries of constraints).

Compared to the CMB anisotropies that allow one to measure ζ accurately in the largest ~ 7 e -folds of scales in the observable Universe, PBHs only provide upper bounds on $\beta(M)$, and hence on ζ . However, these constraints span a much larger range of scales and therefore yield valuable additional information. This is why PBHs can be used to constrain the shape of the inflationary potential beyond the ~ 7 e -folds that are accessible through the CMB.

In practice, one usually assumes $P(\zeta_{\text{cg}})$ to be a Gaussian PDF with standard deviation given by the integrated power spectrum $\langle \zeta_{\text{cg}}^2 \rangle = \int_k^{k_{\text{end}}} \mathcal{P}_\zeta(\tilde{k}) d \ln \tilde{k}$, where k is related to the time of formation through $k = aH_{\text{form}}$, and where k_{end} corresponds to the wavenumber that exits the Hubble radius at the end of inflation. Combined with Eq. (1.1), this gives rise to

$$\beta(M) = \text{erfc} \left[\frac{\zeta_c}{\sqrt{2 \int_k^{k_{\text{end}}} \mathcal{P}_\zeta(\tilde{k}) d \ln \tilde{k}}} \right], \quad (1.3)$$

where erfc is the complementary error function, M is the mass contained in the Hubble volume, and $2\pi/k$ is the comoving Hubble length when the black holes form. In the limit $\beta \ll 1$, this leads to $\int_k^{k_{\text{end}}} \mathcal{P}_\zeta(\tilde{k}) d \ln \tilde{k} \simeq \zeta_c^2 / (-2 \ln \beta)$. Assuming the power spectrum to

be scale invariant, one has $\int_k^{k_{\text{end}}} \mathcal{P}_\zeta(\tilde{k}) d \ln \tilde{k} \simeq \mathcal{P}_\zeta \ln(k_{\text{end}}/k) \simeq \mathcal{P}_\zeta \Delta N$, where $\Delta N = \Delta \ln a$ is the number of e -folds elapsed between the Hubble radius exit times of k and k_{end} during inflation. This leads to

$$\mathcal{P}_\zeta \Delta N \simeq -\frac{\zeta_c^2}{2 \ln \beta}. \quad (1.4)$$

For instance, with $\zeta_c = 1$, the bound $\beta < 10^{-22}$ leads to the requirement that $\mathcal{P}_\zeta \Delta N < 10^{-2}$. This can be translated into constraints on the inflationary potential $V = 24\pi^2 M_{\text{Pl}}^4 v$ and its derivative V' with respect to the inflaton field ϕ using the slow-roll formulae [27, 28]

$$\mathcal{P}_\zeta = \frac{2v^3}{M_{\text{Pl}}^2 v'^2}, \quad \Delta N = \int_{\phi_{\text{end}}}^{\phi} \frac{v}{M_{\text{Pl}}^2 v'} d\tilde{\phi}. \quad (1.5)$$

The crucial remark that motivates the present work is that the assumptions on which the above considerations rely, namely the use of a Gaussian PDF for $P(\zeta_{\text{cg}})$ together with the classical slow-roll formula for the curvature power spectrum \mathcal{P}_ζ and number of e -folds ΔN , are valid only in the regime where quantum diffusion provides a subdominant correction to the classical field dynamics during inflation. However, as we shall now see, producing curvature fluctuations of order $\zeta \sim \zeta_c \sim 1$ or higher precisely corresponds to the regime where quantum diffusion dominates the field dynamics over a typical time scale of one e -fold. The validity of the standard approach that is summarised above is therefore questionable and this is why in this paper, we present a generic calculation of the PBH abundance from inflation that fully incorporates quantum backreaction effects, and we update Eq. (1.4) to take into account the full quantum dynamics of the inflaton field.

In practice, we make use of the stochastic inflation formalism [29–37], which is an effective theory for the long-wavelength parts of the quantum fields during inflation. When light fields are coarse grained at a fixed, non-expanding, physical scale that is larger than the Hubble radius during the whole period of inflation, one can show that their dynamics indeed become classical and stochastic. In the slow-roll approximation, the inflaton field ϕ follows a Langevin equation of the form

$$\frac{d\phi}{dN} = -\frac{V'}{3H^2} + \frac{H}{2\pi} \xi(N). \quad (1.6)$$

The right-hand side of this equation has two terms, the first of which involves V' and is a classical drift term, and the second term involves ξ which is a Gaussian white noise such that $\langle \xi(N) \rangle = 0$ and $\langle \xi(N) \xi(N') \rangle = \delta(N - N')$, and which makes the dynamics stochastic.

Over the time scale of one e -fold, the ratio between the mean quantum kick, $H/(2\pi)$, and the classical drift, $V'/(3H^2)$, is of order $\sqrt{\mathcal{P}_\zeta}$, provided \mathcal{P}_ζ follows the classical formula (1.5) and where one has made use of the Friedmann slow-roll equation $H^2 \simeq 8\pi^2 M_{\text{Pl}}^2 v$. Therefore, if PBHs form when this ratio is of order one or higher, this is precisely when one expects quantum modifications to the standard result to become important.

The effects of quantum diffusion on PBHs formation can thus be dramatic and are the subject of this paper, which is organised as follows. In Sec. 2, we explain how the full PDF of curvature perturbations can be calculated in stochastic inflation. Using the stochastic- δN formalism (see Sec. 2.1), we first derive a set of ordinary differential equations for the moments of this PDF (see Sec. 2.2), from which two methods of construction of the distribution are proposed, one based on its characteristic function (see Sec. 2.3) and one based on a heat equation (see Sec. 2.4). In Sec. 3, we derive the classical limit of our formulation, where quantum diffusion is a subdominant correction to the classical field dynamics. At leading order, the standard result is recovered, and higher-order corrections allow us to calculate the first non-Gaussian modifications to the PDF of curvature perturbations and to the mass fraction β . In Sec. 4, we expand our calculation in the opposite limit, where the potential is exactly flat and stochastic effects dominate. In this case, the PDF of curvature perturbations is found to be highly non-Gaussian and is given by an elliptic theta function. In Sec. 5, we explain how these two limits enable one to treat more generic inflationary potentials and give a simple calculational programme that updates Eq. (1.4) and allows one to translate PBH observational constraints into constraints on the potential. We then illustrate this programme with two examples. We finally summarise our main results and present our conclusions in Sec. 6.

2 Probability distribution of curvature perturbations

The calculation of the PBH mass fraction relies on the PDF of the coarse-grained curvature perturbations through Eq. (1.1). Let us explain how this distribution can be calculated in the stochastic- δN formalism.

2.1 The stochastic- δN formalism

2.1.1 The δN formalism

The starting point of the stochastic- δN formalism is the standard, classical δN formalism [9, 38–42], which provides a succinct way of relating the fluctuations in the number of e -folds of expansion during inflation for a family of homogeneous universes with the statistical properties of curvature perturbations. Starting from the unperturbed flat Friedmann-Lemaître-Robertson-Walker metric

$$ds^2 = -dt^2 + a^2(t)\delta_{ij}dx^i dx^j, \quad (2.1)$$

deviations from isotropy and homogeneity can be added at the perturbative level and contain scalar, vector and tensor degrees of freedom. Gauge redundancies associated with diffeomorphism invariance allow one to choose a specific gauge in which fixed time slices have uniform energy density and fixed spatial worldlines are comoving (in the super-Hubble regime this gauge coincides with the synchronous gauge supplemented by some additional conditions that fix it uniquely). Including spatial perturbations only, one obtains [9, 43, 44]

$$ds^2 = -dt^2 + a^2(t)e^{2\zeta(t,\mathbf{x})}\delta_{ij}dx^i dx^j, \quad (2.2)$$

where ζ is the adiabatic curvature perturbation mentioned in Sec. 1. One can then introduce a local scale factor

$$\tilde{a}(t, \mathbf{x}) = a(t)e^{\zeta(t, \mathbf{x})}, \quad (2.3)$$

which allows us to express the amount of expansion from an initial flat space-time slice at time t_{in} to a final space-time slice of uniform energy density as

$$N(t, \mathbf{x}) = \ln \left[\frac{\tilde{a}(t, \mathbf{x})}{a(t_{\text{in}})} \right]. \quad (2.4)$$

This is related to the curvature perturbation ζ via Eq. (2.3), which gives rise to

$$\zeta(t, \mathbf{x}) = N(t, \mathbf{x}) - \bar{N}(t) \equiv \delta N, \quad (2.5)$$

where $\bar{N}(t) \equiv \ln [a(t)/a(t_{\text{in}})]$ is the unperturbed expansion. This expression forms the basis of the δN formalism, which follows by making the further simplifying assumption that on super-Hubble scales, each spatial point of the universe evolves independently and this evolution is well approximated by the evolution of an unperturbed universe. This assumption is known as the “quasi-isotropic” [45–48] or “separate universe” approach [41, 49, 50], and allows us to neglect spatial gradients on super-Hubble scales. As a consequence, $N(t, \mathbf{x})$ is the amount of expansion in unperturbed, homogeneous universes, and ζ can be calculated from the knowledge of the evolution of a family of such universes.

2.1.2 The stochastic- δN formalism

The δN formalism relies on the calculation of the amount of expansion realised amongst a family of homogeneous universes. When stochastic inflation is employed to describe such a family of universes and to calculate the amount of expansion realised in them, this gives rise to the stochastic- δN formalism [51–57].

This approach is sketched in Fig. 1. Starting from $\phi = \phi_*$ at an initial time, the inflaton field evolves along the potential $v(\phi)$ under the Langevin equation (1.6), where hereafter we use the rescaled dimensionless potential

$$v \equiv \frac{V}{24\pi^2 M_{\text{Pl}}^4}, \quad (2.6)$$

until it reaches ϕ_{end} where inflation ends. A reflective wall is added at ϕ_{uv} to prevent the field from exploring arbitrarily large values, which can be necessary to renormalise infinities appearing in the theory [57] (whose results are still independent of ϕ_{uv} and of the exact nature of the wall, reflective or absorbing, provided ϕ_{uv} lies in some range). The amount of expansion realised along a given trajectory is called \mathcal{N} , which is a stochastic variable. Thanks to the δN formalism, the fluctuation in this number of e -folds, $\mathcal{N} - \langle \mathcal{N} \rangle$, is nothing but the coarse-grained curvature perturbation ζ_{cg} defined in Eq. (1.2),

$$\delta N_{\text{cg}}(\mathbf{x}) = \mathcal{N}(\mathbf{x}) - \langle \mathcal{N} \rangle = \zeta_{\text{cg}}(\mathbf{x}) = \frac{1}{(2\pi)^{3/2}} \int_{k_*}^{k_{\text{end}}} d\mathbf{k} \zeta_{\mathbf{k}} e^{i\mathbf{k}\cdot\mathbf{x}}, \quad (2.7)$$

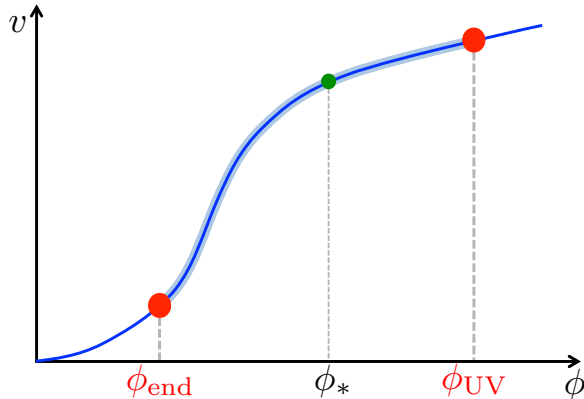


Figure 1. Sketch of the single-field stochastic dynamics solved in this work. Starting from ϕ_* at initial time, the inflaton field ϕ evolved along the potential $v(\phi)$ under the Langevin equation (1.6), until ϕ reaches ϕ_{end} where inflation ends. A reflective wall is added at ϕ_{UV} to prevent the field from exploring arbitrarily large values. The number of e -folds realised along a family of realisations of the Langevin equation is calculated, and gives rise to the probability distribution of curvature perturbations using the δN formalism.

where k_* and k_{end} are the wavenumbers that cross the Hubble radius at initial and final times when $\phi = \phi_*$ and $\phi = \phi_{\text{end}}$ respectively. Since, as explained in Sec. 1, the calculation of the PBH mass function relies on the PDF of coarse-grained curvature perturbations, the next step is to calculate the PDF of δN_{cg} .

Before doing so, let us note that quantities related to ζ , and not ζ_{cg} , can also be calculated in the stochastic- δN formalism. For the power spectrum \mathcal{P}_ζ for instance, since the coarse-grained δN_{cg} receives an integrated contribution of all modes exiting the Hubble radius during inflation, $\langle \delta N_{\text{cg}}^2 \rangle = \int_{k_*}^{k_{\text{end}}} \mathcal{P}_\zeta dk/k$, one has [52, 54]

$$\mathcal{P}_\zeta = \frac{d \langle \delta N_{\text{cg}}^2 \rangle}{d \langle \mathcal{N} \rangle}, \quad (2.8)$$

where we have used the relation $\langle \mathcal{N} \rangle = \ln(a_{\text{end}}/a_*) = \ln(k_{\text{end}}/k)$, where the last equality is valid at leading order in slow roll only. In the same manner, the local bispectrum can be written as $\mathcal{B}_\zeta \propto d^2 \langle \delta N_{\text{cg}}^3 \rangle / d \langle \mathcal{N} \rangle^2$, from which the effective $f_{\text{NL}}^{\text{local}}$ parameter, measuring the ratio between the bispectrum and the power spectrum squared, is given by

$$f_{\text{NL}}^{\text{local}} = \frac{5}{72} \frac{\langle \delta N_{\text{cg}}^3 \rangle}{d \langle \mathcal{N} \rangle^2} \left(\frac{d \langle \delta N_{\text{cg}}^2 \rangle}{d \langle \mathcal{N} \rangle} \right)^{-2}. \quad (2.9)$$

2.2 Statistical moments of first passage times

In order to calculate the PDF of the realised number of e -folds \mathcal{N} , and hence of δN_{cg} (i.e. of ζ_{cg}), a first step consists in calculating its statistical moments

$$f_n(\phi) = \langle \mathcal{N}^n(\phi) \rangle, \quad (2.10)$$

where the dependence on the field value ϕ (denoted ϕ_* in the discussion around Fig. 1) at which trajectories are initiated is made explicit. This can be done using the techniques of “first passage time analysis” [58, 59], applied to stochastic inflation in Refs. [29, 54], which allow one to derive a hierarchy of ordinary differential equations

$$f_n'' - \frac{v'}{v^2} f_n' = -\frac{n}{v M_{\text{Pl}}^2} f_{n-1}. \quad (2.11)$$

The hierarchy is initiated at $f_0 = 1$, and for $n \geq 1$ it has to be solved with two boundary conditions, one related to the fact that all trajectories initiated at ϕ_{end} realise a vanishing number of e -folds, and the other one implementing the presence of a reflective wall at ϕ_{uv} , namely

$$f_n(\phi_{\text{end}}) = 0, \quad f_n'(\phi_{\text{uv}}) = 0. \quad (2.12)$$

The formal solution to this problem can be written as

$$f_n(\phi) = n \int_{\phi_{\text{end}}}^{\phi} \frac{dx}{M_{\text{Pl}}} \int_x^{\phi_{\text{uv}}} \frac{dy}{M_{\text{Pl}}} e^{\frac{1}{v(y)} - \frac{1}{v(x)}} \frac{f_{n-1}(y)}{v(y)}, \quad (2.13)$$

which allows one to calculate the moments iteratively. In practice, this relies on performing integrals of increasing dimension, which quickly becomes numerically heavy but provides a convenient way to study the first few moments required to calculate the power spectrum given by Eq. (2.8) or the $f_{\text{NL}}^{\text{local}}$ parameter given by Eq. (2.9), see Refs. [54, 57].

2.3 The characteristic function approach

In order to relate the PDF of \mathcal{N} to its statistical moments, let us introduce its characteristic function

$$\chi_{\mathcal{N}}(t, \phi) \equiv \langle e^{it\mathcal{N}(\phi)} \rangle, \quad (2.14)$$

which depends on ϕ and a dummy parameter t . By Taylor expanding $\chi_{\mathcal{N}}(t, \phi)$ around $t = 0$, one has $\chi_{\mathcal{N}}(t, \phi) = \sum_{n=0}^{\infty} (it)^n f_n(\phi)/n!$. If one applies the differential operator appearing in the left-hand side of Eq. (2.11) to this expansion, and uses Eq. (2.11) to replace each term by its right-hand side, one obtains

$$\left(\frac{\partial^2}{\partial \phi^2} - \frac{v'}{v^2} \frac{\partial}{\partial \phi} + \frac{it}{v M_{\text{Pl}}^2} \right) \chi_{\mathcal{N}}(t, \phi) = 0. \quad (2.15)$$

At fixed t , this is an ordinary differential equation in ϕ , so instead of the hierarchy of coupled differential equations (2.11) one now has a set of uncoupled differential equations

to solve, which improves the tractability of the problem. The boundary conditions (2.12), together with the fact that $f_0 = 1$, translate into

$$\chi_{\mathcal{N}}(t, \phi_{\text{end}}) = 1, \quad \frac{\partial \chi_{\mathcal{N}}}{\partial \phi}(t, \phi_{\text{uv}}) = 0. \quad (2.16)$$

Let us note that the characteristic function of the fluctuation in the number of e -folds, $\zeta_{\text{cg}} = \delta N_{\text{cg}} = \mathcal{N} - \langle \mathcal{N} \rangle = \mathcal{N} - f_1$, can be found by plugging this expression into Eq. (2.14), which gives rise to

$$\chi_{\zeta_{\text{cg}}}(t, \phi) = e^{-if_1(\phi)t} \chi_{\mathcal{N}}(t, \phi). \quad (2.17)$$

Finally, from Eq. (2.14), the characteristic function $\chi_{\mathcal{N}}$ can be rewritten as

$$\chi_{\mathcal{N}}(t, \phi) = \int_{-\infty}^{\infty} e^{it\mathcal{N}} P(\mathcal{N}, \phi) d\mathcal{N}, \quad (2.18)$$

that is to say, the characteristic function is the Fourier transform of the PDF of curvature perturbations. Therefore, the PDF is the inverse Fourier transform of the characteristic function, i.e.

$$P(\zeta_{\text{cg}}, \phi) = \frac{1}{2\pi} \int_{-\infty}^{\infty} e^{-it[\zeta_{\text{cg}} + f_1(\phi)]} \chi_{\mathcal{N}}(t, \phi) dt, \quad (2.19)$$

where we have used Eq. (2.17). The calculational programme is thus the following: solve Eq. (2.15) with boundary conditions (2.16), calculate f_1 either taking $n = 1$ and $f_0 = 1$ in Eq. (2.13) or by noting that $f_1(\phi) = -i\partial\chi_{\mathcal{N}}/\partial t(t = 0, \phi)$, calculate the PDF of curvature perturbations with Eq. (2.19), and then the mass fraction of PBHs with Eq. (1.1).

Example: quadratic potential

In order to illustrate this computational programme, let us consider the case of a quadratic potential

$$v(\phi) = v_0 \left(\frac{\phi}{M_{\text{Pl}}} \right)^2. \quad (2.20)$$

In this case, Eq. (2.15) together with the boundary conditions (2.16) has an exact solution. Taking the $\phi_{\text{uv}} \rightarrow \infty$ limit, it is given by

$$\chi_{\mathcal{N}}(t, \phi) = \left[\frac{v(\phi)}{v(\phi_{\text{end}})} \right]^{\frac{1-\alpha(t)}{4}} \frac{{}_1F_1 \left[\frac{\alpha(t)-1}{4}; 1 + \frac{\alpha(t)}{2}; -\frac{1}{v(\phi)} \right]}{{}_1F_1 \left[\frac{\alpha(t)-1}{4}; 1 + \frac{\alpha(t)}{2}; -\frac{1}{v(\phi_{\text{end}})} \right]}, \quad (2.21)$$

where $\alpha(t) = \sqrt{1 - \frac{4it}{v_0}}$ and ${}_1F_1(x; y; z)$ is the Kummer confluent hypergeometric function [60, 61]¹. The inverse Fourier transform of Eq. (2.21) can then be computed numerically, which gives rise to the PDF displayed in Fig. 2. At small $v(\phi)$ the PDF is

¹Note that these references use the notation $M(a, b, z)$ for the Kummer confluent hypergeometric function while we use the notation ${}_1F_1$.

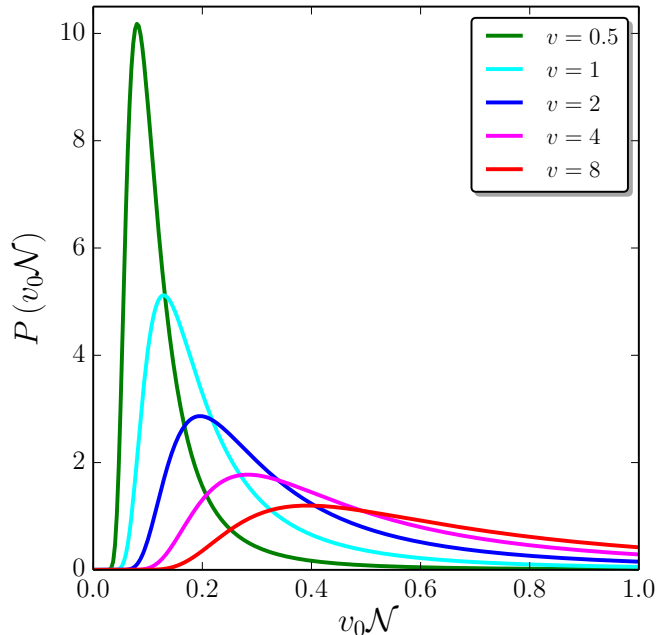


Figure 2. Probability distributions of the number of e -folds \mathcal{N} , rescaled by v_0 , realised in the quadratic potential (2.20) between an initial field value ϕ parametrised by $v(\phi)$ given in the legend, and $\phi_{\text{end}} = \sqrt{2} M_{\text{Pl}}$ where inflation ends by slow-roll violation. The values displayed for v correspond to very high energies far from the observational window of this model but this is for illustrative purpose only. When v increases, one can see that the PDF has a larger mean value, a larger spread and seems to be less Gaussian, which motivates the need to go beyond Gaussian techniques.

rather peaked and almost Gaussian, while at large $v(\phi)$, it is more spread and deviates more from a Gaussian distribution. In Secs. 3 and 4 we will study these two limits one by one, i.e. the classical limit where the stochastic corrections are small and the PDF is almost Gaussian, and the stochastic limit where quantum diffusion dominates the inflaton dynamics.

2.4 The heat equation approach

Before investigating the classical and stochastic limits, let us note that the problem can be reformulated in terms of a heat equation for the PDF $P(\mathcal{N}, \phi)$. Indeed, if one plugs Eq. (2.18) into Eq. (2.15), the two first terms apply on $P(\mathcal{N}, \phi)$ directly, while the third one is given by $it\chi_{\mathcal{N}} = \int_{-\infty}^{\infty} d\mathcal{N} P(\mathcal{N}, \phi) \partial e^{it\mathcal{N}} / \partial \mathcal{N} = - \int_{-\infty}^{\infty} d\mathcal{N} e^{it\mathcal{N}} \partial P / \partial \mathcal{N}(\mathcal{N}, \phi)$. Here, in the first expression, we have simply differentiated Eq. (2.18) with respect to \mathcal{N} , and in the second expression, we have integrated by parts (the boundary terms vanish since $P(\mathcal{N} = \pm\infty, \phi)$ must vanish for the distribution to be normalisable). This gives

rise to the heat equation

$$\left(\frac{\partial^2}{\partial \phi^2} - \frac{v'}{v^2} \frac{\partial}{\partial \phi} - \frac{1}{v M_{\text{Pl}}^2} \frac{\partial}{\partial \mathcal{N}} \right) P(\mathcal{N}, \phi) = 0. \quad (2.22)$$

Instead of the infinite set of uncoupled differential equations given in Eq. (2.15), the problem is now reformulated in terms of a single, but partial, differential equation. Let us note that Eq. (2.22) does not have the structure of a Fokker-Planck equation, and should in any case not be confused with the usual Fokker-Planck equation considered in stochastic inflation which governs the PDF of the field value.² When plugging the boundary conditions (2.16) into Eq. (2.18), one obtains

$$P(\mathcal{N}, \phi_{\text{end}}) = \delta(\mathcal{N}), \quad \frac{\partial P}{\partial \phi}(\mathcal{N}, \phi_{\text{uv}}) = 0. \quad (2.24)$$

These form the boundary conditions associated to Eq. (2.22).

In order to show that Eq. (2.22) has the structure of a heat equation as announced above, one can introduce a change of field variable

$$u(\phi) = \int_{\phi_{\text{end}}}^{\phi} e^{-\frac{1}{v(\tilde{\phi})}} \frac{d\tilde{\phi}}{M_{\text{Pl}}}, \quad (2.25)$$

which allows us to rewrite Eq. (2.22) as

$$\left(v e^{-\frac{2}{v}} \frac{\partial^2}{\partial u^2} - \frac{\partial}{\partial \mathcal{N}} \right) P(\mathcal{N}, u) = 0. \quad (2.26)$$

This is a heat equation for a one dimensional medium with diffusivity $v e^{-2/v}$, where \mathcal{N} plays the role of time and u the role of space. However, let us stress that heat equations are usually endowed with boundary conditions of a different type as from those in Eq. (2.24), since in standard heat equations, one usually gives the spatial temperature distribution at an initial time, while Eq. (2.24) involves distributions of times at fixed spatial positions. This is why the numerical methods developed in the literature to solve heat equations would need to be adapted to this kind of boundary conditions but they may provide efficient ways to solve the problem at hand, e.g. , in the context of multi-field inflation.

²The Langevin equation (1.6) gives rise to Fokker-Planck equation for the probability density $p(N, \phi)$ of the field to be at ϕ at time N , which, in the Itô interpretation, is given by

$$\frac{\partial^2}{\partial \phi^2} [v p(N, \phi)] + \frac{\partial}{\partial \phi} \left[\frac{v'}{v} p(N, \phi) \right] - \frac{1}{M_{\text{Pl}}^2} \frac{\partial}{\partial N} p(N, \phi) = 0. \quad (2.23)$$

This equation does not coincide with Eq. (2.22) for $P(\mathcal{N}, \phi)$ which governs the probability to realise \mathcal{N} e -folds starting from ϕ .

3 Expansion about the classical limit

In the limit of small quantum diffusion, the “classical” limit, one needs to check that our formulation allows one to recover the standard results recalled in Sec. 1 around Eq. (1.3). This is the goal of this section, where we also calculate the leading order deviation from the standard result in order to best determine its range of validity. From the heat equation (2.26), we saw that the diffusivity increases with v , which implies that the classical limit has $v \ll 1$ (this condition is not enough to define the classical regime as we will see below but it constitutes a fair starting point). We thus perform an expansion in increasing powers of v , first in the characteristic function approach introduced in Sec. 2.3, and then in the heat equation approach introduced in Sec. 2.4. We will see that the former is much more convenient than the later which only yields limited results in the classical limit.

3.1 The characteristic function approach

In the ordinary differential equation satisfied by the characteristic function, Eq. (2.15), an expansion in v is equivalent to an expansion in the diffusion term, involving $\partial^2/\partial\phi^2$.

3.1.1 Leading order

At leading order (LO) in the classical limit, the diffusion term in Eq. (2.15) can be simply neglected, and one has

$$\left(-\frac{v'}{v}\frac{\partial}{\partial\phi} + \frac{it}{M_{\text{P1}}^2}\right)\chi_{\mathcal{N}}^{\text{LO}}(t, \phi) = 0. \quad (3.1)$$

Making use of the first boundary condition in Eq. (2.16),³ this equation can be solved as

$$\chi_{\mathcal{N}}^{\text{LO}}(t, \phi) = \exp\left[it\int_{\phi_{\text{end}}}^{\phi}\frac{v(x)}{M_{\text{P1}}^2 v'(x)}dx\right]. \quad (3.2)$$

Note that the integral in the argument of the exponential is the classical number of e -folds, which is also the mean number of e -folds at leading order in the classical limit, i.e. the leading order saddle point expansion of Eq. (2.13) [57],

$$f_1^{\text{LO}}(\phi) = \frac{1}{M_{\text{P1}}^2}\int_{\phi_{\text{end}}}^{\phi}\frac{v(x)}{v'(x)}dx. \quad (3.3)$$

This is consistent with the formula given below Eq. (2.19), namely $f_1(\phi) = -i\partial\chi_{\mathcal{N}}/\partial t(t=0, \phi)$. As a consequence, Eq. (2.17) implies that $\chi_{\delta N_{\text{cg}}} = 1$, and hence its inverse Fourier transform is $P^{\text{LO}}(\delta N_{\text{cg}}, \phi) = \delta(\delta N_{\text{cg}})$, i.e. a Dirac distribution centred around $\delta N_{\text{cg}} = 0$. Thus, at leading order in the classical limit, one simply shuts down quantum diffusion, the dynamics are purely deterministic, $\delta\mathcal{N} \equiv 0$ and there are no curvature perturbations.

³In the expansion about the classical limit, the second boundary condition in Eq. (2.16) cannot be satisfied simultaneously with the first condition. This is why the solutions presented here are, strictly speaking, only valid in the limit $\phi_{\text{uv}} \rightarrow \infty$.

3.1.2 Next-to-leading order

One thus needs to go to next-to-leading order (NLO) to incorporate curvature perturbations. At NLO, the LO solution (3.2) can be used to evaluate the term $\chi^{-1}\partial^2\chi/\partial\phi^2$ in Eq. (2.15), which then becomes

$$\frac{\partial}{\partial\phi}\chi_{\mathcal{N}}^{\text{NLO}} - \frac{v^2}{v'}\left(\frac{it}{vM_{\text{Pl}}^2} + \frac{1}{\chi_{\mathcal{N}}^{\text{LO}}}\frac{\partial^2\chi_{\mathcal{N}}^{\text{LO}}}{\partial\phi^2}\right)\chi_{\mathcal{N}}^{\text{NLO}} = 0. \quad (3.4)$$

Making use of the first boundary condition in Eq. (2.16), the solution of this first order ordinary differential equation is

$$\chi_{\mathcal{N}}^{\text{NLO}}(t, \phi) = \exp\left\{\int_{\phi_{\text{end}}}^{\phi}\left[\frac{itv(x)}{M_{\text{Pl}}^2v'(x)} + \frac{v^2(x)}{v'(x)}\frac{1}{\chi_{\mathcal{N}}^{\text{LO}}(x)}\frac{\partial^2\chi_{\mathcal{N}}^{\text{LO}}}{\partial\phi^2}(x)\right]dx\right\}. \quad (3.5)$$

Notice that if ones replaces $_{\text{LO}}$ by an arbitrary n^{th} order and $_{\text{NLO}}$ by the $n+1^{\text{th}}$ order of the classical expansion, this equation is valid at any order since it is nothing but the iterative solution of Eq. (2.15). At NLO, plugging Eq. (3.2) into Eq. (3.5), one obtains

$$\chi_{\mathcal{N}}^{\text{NLO}}(t, \phi) = \exp\left[itf_1^{\text{NLO}}(\phi) - \gamma_1^{\text{NLO}}vt^2\right], \quad (3.6)$$

where f_1^{NLO} is the mean number of e -folds at NLO [57],

$$f_1^{\text{NLO}}(\phi) = \frac{1}{M_{\text{Pl}}^2}\int_{\phi_{\text{end}}}^{\phi}dx\left(\frac{v}{v'} + \frac{v^2}{v'} - \frac{v^3v''}{v'^3}\right), \quad (3.7)$$

and we have defined

$$\gamma_1^{\text{NLO}} = \frac{1}{vM_{\text{Pl}}^4}\int_{\phi_{\text{end}}}^{\phi}dx\frac{v^4}{v'^3}. \quad (3.8)$$

From this expression, Eq. (2.17) implies that $\chi_{\delta N_{\text{cg}}}^{\text{NLO}}(t, \phi) = e^{-\gamma_1^{\text{NLO}}vt^2}$, that is to say $\chi_{\delta N}^{\text{NLO}}$ is a Gaussian and hence its inverse Fourier transform $P^{\text{NLO}}(\zeta_{\text{cg}}, \phi)$ is also a Gaussian and is given by

$$P^{\text{NLO}}(\zeta_{\text{cg}}, \phi) = \frac{1}{\sqrt{4\pi\gamma_1^{\text{NLO}}v}}\exp\left(-\frac{\zeta_{\text{cg}}^2}{4\gamma_1^{\text{NLO}}v}\right). \quad (3.9)$$

A crucial remark is that at this order, the power spectrum (2.8) is given by [54] Eq. (1.5), so that the variance of the Gaussian distribution (3.9) reads $2\gamma_1^{\text{NLO}}v = \int_{\phi_{\text{end}}}^{\phi}\mathcal{P}_{\zeta}^{\text{NLO}}f_1^{\text{LO}}dx$. This precisely matches the standard result recalled above Eq. (1.3), namely that $P(\zeta_{\text{cg}})$ is a Gaussian PDF with standard deviation given by the integrated power spectrum $\langle\zeta_{\text{cg}}^2\rangle = \int_k^{k_{\text{end}}}\mathcal{P}_{\zeta}(\tilde{k})d\ln\tilde{k}$, since $d\ln k \simeq dN = f_1'(\phi)d\phi$ at leading order in slow roll.

3.1.3 Next-to-next-to-leading order

In order to study the first non-Gaussian corrections to the standard result, one needs to go to next-to-next-to-leading order (NNLO). As explained in Sec. 3.1.2, one can simply

increment the order of the iterative relation (3.5), i.e. replace LO by NLO and NLO by NNLO . Plugging in Eq. (3.6), and making use of Eq. (2.17), this gives rise to

$$\chi_{\delta N_{\text{cg}}}^{\text{NNLO}}(t, \phi) = \exp\left(-\gamma_1^{\text{NNLO}} v t^2 - i\gamma_2^{\text{NNLO}} v^2 t^3\right), \quad (3.10)$$

where we have only kept the terms that are consistent at that order and where we have defined

$$\begin{aligned} \gamma_1^{\text{NNLO}} &= \frac{1}{v M_{\text{Pl}}^4} \int_{\phi_{\text{end}}}^{\phi} dx \left(\frac{v^4}{v'^3} + 6 \frac{v^5}{v'^3} - 5 \frac{v^6 v''}{v'^5} \right), \\ \gamma_2^{\text{NNLO}} &= \frac{2}{v^2 M_{\text{Pl}}^6} \int_{\phi_{\text{end}}}^{\phi} dx \frac{v^7}{v'^5}. \end{aligned} \quad (3.11)$$

One can already see that since the characteristic function is not a Gaussian, the PDF is not a Gaussian distribution. Using Eq. (2.19), it is given by

$$P^{\text{NNLO}}(\delta N_{\text{cg}}, \phi) = \frac{1}{2\pi} \int_{-\infty}^{\infty} dt \exp\left(-it\delta N_{\text{cg}} - \gamma_1^{\text{NNLO}} v t^2 + i\gamma_2^{\text{NNLO}} v^2 t^3\right). \quad (3.12)$$

In this integral, the second term in the argument of the exponential makes the integrand become negligible when $\gamma_1^{\text{NNLO}} v t^2 \gg 1$, i.e. for $|t| \gg t_c$ where $t_c = (\gamma_1^{\text{NNLO}} v)^{-1/2}$. When $t = \pm t_c$, the ratio between the third and the second terms in the argument of the exponential of Eq. (3.12) is of order $(\gamma_2^{\text{NNLO}}/\gamma_1^{\text{NNLO}}) \sqrt{v/\gamma_1^{\text{NNLO}}}$, i.e. of order \sqrt{v} in an expansion in v since the γ_i parameters have been defined to carry no dimension of v (at least at their leading orders). This is why, over the domain of integration where most of the contribution to the integral comes from, the third term is negligible and can be Taylor expanded. One obtains

$$P^{\text{NNLO}}(\zeta_{\text{cg}}, \phi) = \frac{1}{\sqrt{4\pi\gamma_1^{\text{NNLO}} v}} \exp\left(-\frac{\zeta_{\text{cg}}^2}{4\gamma_1^{\text{NNLO}} v}\right) \left[1 - \frac{\gamma_2^{\text{NNLO}}}{8(\gamma_1^{\text{NNLO}})^3 v} \zeta_{\text{cg}} (6\gamma_1^{\text{NNLO}} v - \zeta_{\text{cg}}^2) \right]. \quad (3.13)$$

For the quadratic potential example discussed in Sec. 2.3, in Fig. 3 we have reproduced Fig. 2 (for different values of v to better illustrate the behaviours of the classical approximations) where we have superimposed the NLO approximation (3.9) and the NNLO approximation (3.13). One can check that these approximations become better at smaller values of v as expected, and that the NNLO approximation always provides a better fit than the NLO one.

As a consistency check, one can verify that the distribution (3.13) yields the same moments at NNLO order as the ones derived in Ref. [54] by calculating the integrals (2.13) with a saddle-point approximation technique at NNLO. For the second moment, one has $\langle \delta N_{\text{cg}}^2 \rangle = \int_{-\infty}^{\infty} \zeta_{\text{cg}}^2 P^{\text{NNLO}}(\zeta_{\text{cg}}, \phi) d\zeta_{\text{cg}} = 2\gamma_1^{\text{NNLO}} v$, which coincides with Eq. (3.35) of Ref. [54]. Similarly for the third moment, $\langle \delta N_{\text{cg}}^3 \rangle = \int_{-\infty}^{\infty} \zeta_{\text{cg}}^3 P^{\text{NNLO}}(\zeta_{\text{cg}}, \phi) d\zeta_{\text{cg}} = 6\gamma_2^{\text{NNLO}} v^2$, which coincides with Eq. (3.37) of Ref. [54]. The two methods, i.e. the iterative solution (3.5) of the characteristic function equation and the saddle-point expansion of the integrals (2.13), are therefore equivalent.

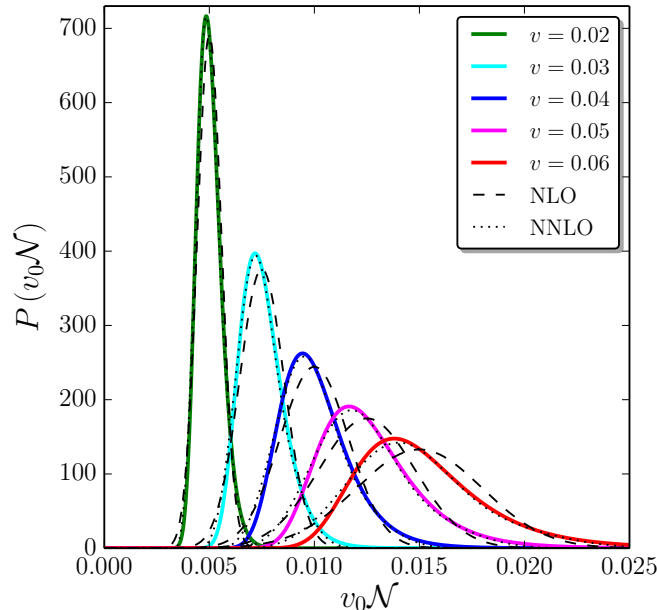


Figure 3. Probability distributions of the number of e -folds \mathcal{N} , rescaled by v_0 , realised in the quadratic potential (2.20) between an initial field value ϕ parametrised by $v(\phi)$ given in the legend, and $\phi_{\text{end}} = \sqrt{2}M_{\text{Pl}}$ where inflation ends by slow-roll violation, as in Fig. 2. The black dashed lines correspond to the NLO (Gaussian) approximation (3.9), while the dotted lines stand for the NNLO approximation (3.13). The smaller v is, the better these approximations are, and the NNLO approximation is substantially better than the NLO one.

Let us also note that the characteristic function, $\chi_{\mathcal{N}}(t, \phi)$ defined in Eq. (2.14), is closely related to the cumulant generating function for the probability distribution

$$K_{\mathcal{N}}(\tau, \phi) = \ln \langle e^{\tau \mathcal{N}(\phi)} \rangle = \sum_{n=1}^{\infty} \frac{\kappa_n(\phi)}{n!} \tau^n. \quad (3.14)$$

By comparing Eqs. (2.14) and (3.14) indeed, one simply has $\chi_{\mathcal{N}}(t, \phi) = \exp[K_{\mathcal{N}}(it, \phi)]$. If we now compare Eqs. (3.10) and (3.14), we can read off the first cumulants

$$\kappa_2(\phi) = 2v\gamma_1, \quad \kappa_3(\phi) = 6v^2\gamma_2. \quad (3.15)$$

One measure of the deviation from a Gaussian distribution is the skewness of the distribution which is determined by the ratio of these cumulants

$$\gamma_{\text{skew}} \equiv \frac{\kappa_3}{\kappa_2^{3/2}} = \frac{3v^{1/2}\gamma_2}{\sqrt{2}(\gamma_1)^{3/2}}. \quad (3.16)$$

Since γ_2 is non-vanishing at next-to-next-to-leading (and higher) order only, the NNLO term thus represents the first non-Gaussian correction to the standard Gaussian result obtained at NLO in the classical limit.

At this order, the distribution is positively skewed, which is indeed the case for all the distributions displayed in Figs. 2 and 3. One can also note that the parameter introduced below Eq. (3.12), that must be small in order for the classical expansion to be valid at NNLO, exactly coincides with γ_{skew} . The above formulae are therefore correct in the limit $\gamma_{\text{skew}} \ll 1$ only. Finally, the correcting term in the brackets of Eq. (3.13) can be expressed as $\gamma_{\text{skew}} (\zeta_{\text{cg}}^2 / \langle \zeta_{\text{cg}}^2 \rangle)^{3/2}$, where we have used the relation $\langle \delta N_{\text{cg}}^2 \rangle = 2\gamma_1^{\text{NNLO}} v$ given above together with Eq. (3.16). This shows that $\gamma_{\text{skew}} \ll 1$ only ensures the correcting term to be small when ζ_{cg}^2 is of order $\langle \zeta_{\text{cg}}^2 \rangle$, i.e. around the maximum of the distribution. The classical approximation is therefore an expansion about the maximum of the distribution that should be expected to fail in the tail. Since the PBH threshold ζ_c is usually in the far tail of the distribution (in the standard calculation recalled in Sec. 1, at the level of the observational bounds, one has $\langle \zeta_{\text{cg}}^2 \rangle \sim 10^{-2} \ll \zeta_c^2 \sim 1$), one may need to go beyond the classical approximation in such cases.

3.2 The heat equation approach

Before moving on to the stochastic limit, let us briefly explain how the heat equation approach proceeds in the classical limit. At LO, neglecting the diffusion term in Eq. (2.22), one has to solve $M_{\text{Pl}}^2 v' / v \partial P / \partial \phi + \partial P / \partial \mathcal{N} = 0$, with the first boundary condition of Eq. (2.24). Using the method of characteristics to solve first-order partial differential equations, one obtains

$$P^{\text{LO}}(\mathcal{N}, \phi) = \delta[\mathcal{N} - f_1^{\text{LO}}(\phi)] , \quad (3.17)$$

where f_1^{LO} has been defined in Eq. (3.3) and corresponds to the classical number of e -folds, which is also the mean number of e -folds at leading order in the classical limit. One therefore recovers the result of Sec. 3.1.1. At NLO, one can use Eq. (3.17) to calculate the diffusive term in Eq. (2.22) and iterate the procedure. However, by doing so, one has to solve a first-order partial differential equation with a source term that involves derivatives of the Dirac distribution. This makes the solving procedure technically complicated, and we therefore do not pursue this direction further since a simpler way to obtain the solution was already presented in Sec. 3.1. One can already see the benefit of having two solving procedures at hand, which will become even more obvious in what follows.

4 The stochastic limit

We now consider the opposite limit where the inflaton field dynamics are dominated by quantum diffusion. This is the case if the potential is exactly flat, since then the slow-roll classical drift vanishes. We thus consider a potential that is constant between the two values ϕ_{end} and $\phi_{\text{end}} + \Delta\phi_{\text{well}}$, where $\Delta\phi_{\text{well}}$ denotes the width of this “quantum well”. Inflation terminates when the field reaches ϕ_{end} (where either the potential is assumed to become very steep, or a mechanism other than slow-roll violation must be invoked to end inflation), and a reflective wall is located at $\phi_{\text{end}} + \Delta\phi_{\text{well}}$, which can be seen as the point where the dynamics become classically dominated so that the probability for field trajectories to climb up this part of the potential and escape the quantum well can

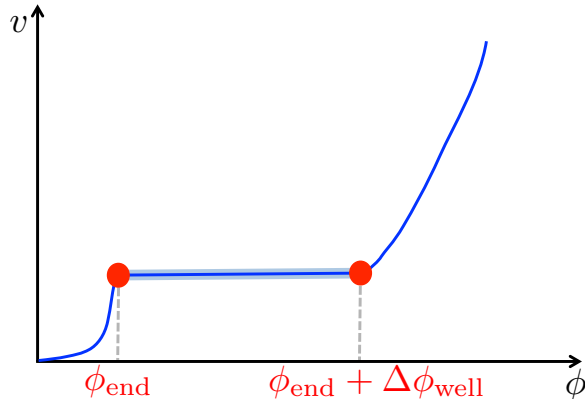


Figure 4. Schematic representation of the single-field stochastic dynamics solved in Sec. 4, where the potential may be taken to be exactly constant over the “quantum well” regime delimited by ϕ_{end} and $\phi_{\text{end}} + \Delta\phi_{\text{well}}$. Inflation terminates at ϕ_{end} , where either the potential becomes very steep or a mechanism other than slow-roll violation ends inflation, and a reflective wall is placed at $\phi_{\text{end}} + \Delta\phi_{\text{well}}$, which can be seen as the point where the dynamics become classically dominated and the classical drift prevents the field from escaping the quantum well.

be neglected. The situation is depicted in Fig. 4, and in Sec. 5 we will see why these assumptions allow one to study most cases of interest.

4.1 The characteristic function approach

If the potential $v = v_0$ is constant, the potential gradient term vanishes in Eq. (2.15) and making use of the boundary conditions (2.16), where ϕ_{uv} is replaced by $\phi_{\text{end}} + \Delta\phi_{\text{well}}$, one obtains

$$\chi_{\mathcal{N}}(t, \phi) = \frac{\cosh[\alpha\sqrt{t}\mu(x-1)]}{\cosh(\alpha\sqrt{t}\mu)}. \quad (4.1)$$

In this expression, $x \equiv (\phi - \phi_{\text{end}})/\Delta\phi_{\text{well}}$, $\alpha \equiv (i-1)/\sqrt{2}$, and we have introduced the parameter

$$\mu^2 = \frac{\Delta\phi_{\text{well}}^2}{v_0 M_{\text{Pl}}^2} \quad (4.2)$$

which is the ratio between the squared width of the quantum well and its height, in Planck mass units, and which is the only combination through which these two quantities appear.

The PDF can be obtained by inverse Fourier transforming Eq. (4.1), see Eq. (2.19), which can be done after Taylor expanding the characteristic function (4.1) and inverse

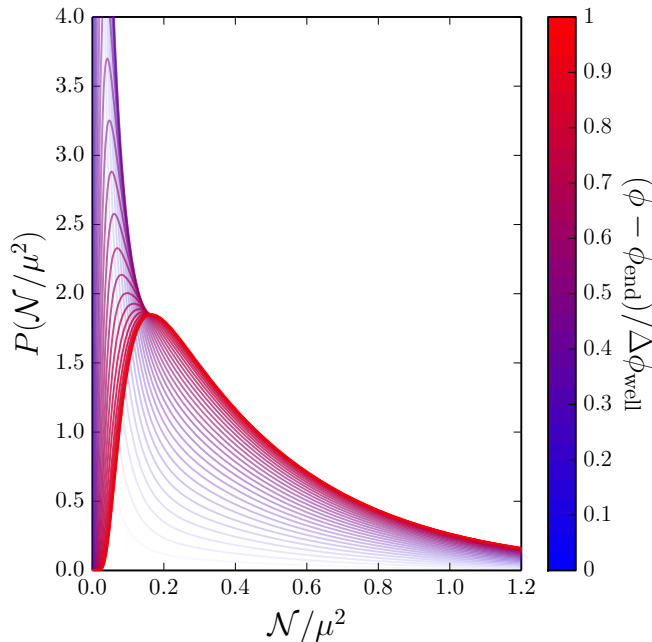


Figure 5. Probability distributions of the number of e -folds \mathcal{N} , rescaled by μ^2 , realised in the constant potential depicted in Fig. 4 between ϕ and ϕ_{end} , where different colours correspond to different values of ϕ . When ϕ approaches ϕ_{end} , the distribution becomes more peaked and the transparency of the curves is increased for displayed purposes.

Fourier transforming each term in the sum. This leads to

$$P(\mathcal{N}, \phi) = \frac{1}{2\sqrt{\pi}} \frac{\mu}{\mathcal{N}^{3/2}} \times \left\{ \sum_{n=0}^{\infty} (-1)^n [2(n+1) - x] e^{-\frac{\mu^2}{4\mathcal{N}} [2(n+1) - x]^2} + \sum_{n=0}^{\infty} (-1)^n [2n + x] e^{-\frac{\mu^2}{4\mathcal{N}} [2n + x]^2} \right\}. \quad (4.3)$$

This PDF is displayed in Fig. 5 for different values of x . Interestingly, Eq. (4.3) can be resummed to give a closed form when combined with the result from the heat equation approach presented below in Sec. 4.2. For now, we can derive closed form expressions at both boundaries of the quantum well, i.e. in the two limits $\phi \simeq \phi_{\text{end}} + \Delta\phi_{\text{well}}$ and $\phi \simeq \phi_{\text{end}}$.

Reflective boundary of the quantum well

In the case where $\phi = \phi_{\text{end}} + \Delta\phi_{\text{well}}$, or $x = 1$, i.e. at the reflective boundary of the quantum well, Eq. (4.3) reduces to $P(\mathcal{N}, \phi_{\text{well}}) = \mu/\sqrt{\pi} \mathcal{N}^{-3/2} \sum_{n=0}^{\infty} (-1)^n (2n+1) e^{-\frac{\mu^2}{4\mathcal{N}} (2n+1)^2}$. Making use of the elliptic theta functions [62, 63] introduced in Ap-

pendix A, this can be rewritten as

$$P(\mathcal{N}, \phi = \phi_{\text{end}} + \Delta\phi_{\text{well}}) = \frac{\mu}{2\sqrt{\pi}\mathcal{N}^{3/2}}\vartheta_1' \left(0, e^{-\frac{\mu^2}{\mathcal{N}}} \right), \quad (4.4)$$

where ϑ_1' is the derivative (with respect to the first argument) of the first elliptic theta function, see Eq. (A.2).

Absorbing boundary of the quantum well

In the case where $\phi \simeq \phi_{\text{end}}$, or $x \ll 1$, i.e. at the absorbing boundary of the quantum well, an approximated formula can be obtained by noting that Eq. (4.3) can be rewritten as $P(\mathcal{N}, \phi) = \mu/(2\sqrt{\pi}\mathcal{N}^{3/2})[xe^{-\mu^2 x^2/(4\mathcal{N})} + F(-x) - F(x)]$, with $F(x) \equiv \sum_{n=0}^{\infty} (-1)^n [2(n+1) + x]e^{-\frac{\mu^2}{4\mathcal{N}}[2(n+1)+x]^2}$. In the limit where $x \ll 1$, $F(-x) - F(x) \simeq -2xF'(0)$, where $F'(0) = 1/2 - 1/2\vartheta_4(0, e^{-\mu^2/\mathcal{N}}) - \mu^2/(4\mathcal{N})\vartheta_4''(0, e^{-\mu^2/4})$, see Eq. (A.3). This gives rise to

$$P(\mathcal{N}, \phi \simeq \phi_{\text{end}}) \simeq \frac{\mu x}{2\sqrt{\pi}\mathcal{N}^{3/2}} \left[e^{-\frac{\mu^2 x^2}{4\mathcal{N}}} - 1 + \vartheta_4 \left(0, e^{-\frac{\mu^2}{\mathcal{N}}} \right) + \frac{\mu^2}{2\mathcal{N}}\vartheta_4'' \left(0, e^{-\frac{\mu^2}{\mathcal{N}}} \right) \right]. \quad (4.5)$$

This approximation is superimposed to the full result (4.4) in the left panel of Fig. 6, where one can check that the agreement is excellent even up to $x \sim 0.3$.

4.2 The heat equation approach

Let us now move on to the heat equation approach, since combined with the results of the characteristic function approach, this will allow us to derive a closed form for the PDF at arbitrary values of x . In the case of a constant potential, the heat equation (2.22) becomes $(v_0 M_{\text{Pl}}^2 \partial^2/\partial\phi^2 - \partial/\partial\mathcal{N})P(\mathcal{N}, \phi) = 0$. The second boundary condition of Eq. (2.24), $\partial P/\partial\phi(\mathcal{N}, \phi_{\text{end}} + \Delta\phi_{\text{well}}) = 0$, leads to a Fourier decomposition of the form

$$P(\mathcal{N}, \phi) = \sum_{n=0}^{\infty} \left\{ A_n(\mathcal{N}) \sin \left[\left(\frac{\pi}{2} + n\pi \right) x \right] + B_n(\mathcal{N}) \cos(n\pi x) \right\}, \quad (4.6)$$

where, by plugging Eq. (4.6) into the heat equation (2.22), the coefficients A_n and B_n must satisfy

$$\frac{\partial A_n}{\partial\mathcal{N}} = -\frac{\pi^2}{\mu^2} \left(n + \frac{1}{2} \right)^2 A_n, \quad \frac{\partial B_n}{\partial\mathcal{N}} = -\frac{\pi^2}{\mu^2} n^2 B_n. \quad (4.7)$$

This leads to

$$A_n(\mathcal{N}) = a_n \exp \left[-\frac{\pi^2}{\mu^2} \left(n + \frac{1}{2} \right)^2 \mathcal{N} \right], \quad B_n(\mathcal{N}) = b_n \exp \left(-\frac{\pi^2}{\mu^2} n^2 \mathcal{N} \right), \quad (4.8)$$

where a_n and b_n are coefficients that depend only on n . They can be calculated by identifying Eqs. (4.3) and (4.6) in the $\mathcal{N} \rightarrow 0$ limit. In this limit, in Eq. (4.3), the term with $n = 0$ of the second sum is the dominant contribution, and using the fact

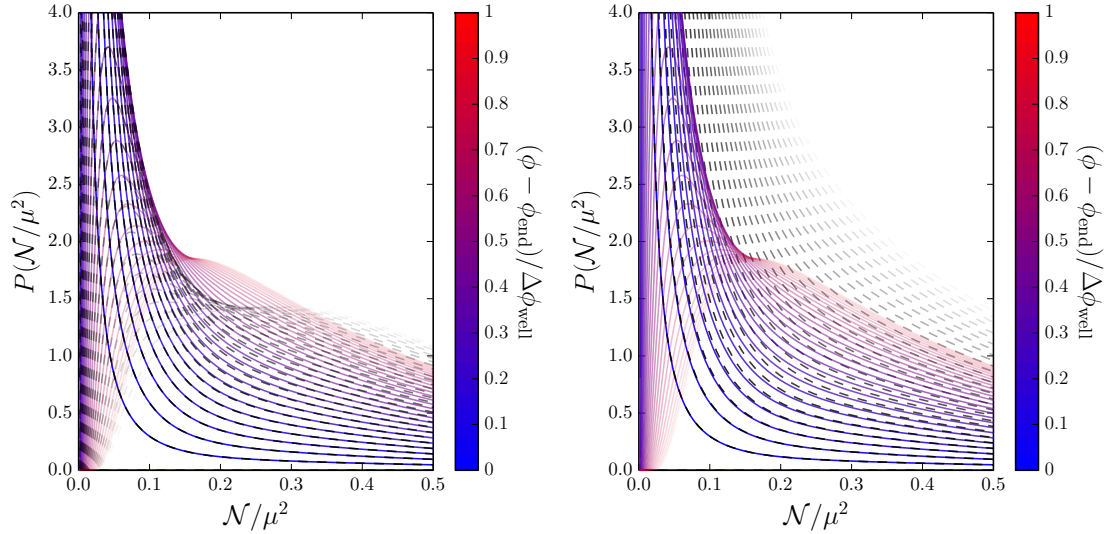


Figure 6. Probability distributions of the number of e -folds \mathcal{N} , rescaled by μ^2 , realised in the constant potential depicted in Fig. 4 between ϕ and ϕ_{end} . In both panels, different colours correspond to different values of ϕ , and the black dashed lines correspond to approximations. Left panel: the approximation (4.5) is displayed with the black dashed lines. Right panel: the approximation (4.12) is displayed with the black dashed lines. These approximations are valid close to the absorbing boundary of the quantum well where inflation ends. When ϕ increases, the approximation becomes worse, and the transparency of the curves is increased for displayed purposes, but one can see that the approximation (4.5) is excellent up to $(\phi - \phi_{\text{end}})/\Delta\phi_{\text{well}} \sim 0.3$, and slightly better than the approximation (4.12).

that $e^{-x^2/(4\sigma)}/(2\sqrt{\pi\sigma}) \rightarrow \delta(x)$ when $\sigma \rightarrow 0$, hence $-xe^{-x^2/(4\sigma)}/(4\sigma\sqrt{\pi\sigma}) \rightarrow \delta'(x)$ when $\sigma \rightarrow 0$, one has

$$P(\mathcal{N}, \phi) \xrightarrow{\mathcal{N} \rightarrow 0} -2v_0 M_{\text{Pl}}^2 \delta'(\phi - \phi_{\text{end}}). \quad (4.9)$$

In passing, one notes that this expression implies that $P(\mathcal{N} = 0, \phi) = 0$ when $\phi \neq \phi_{\text{end}}$, which is consistent with the continuity of the distribution when $\mathcal{N} = 0$ and with the fact that the probability to realise a negative number of e -folds obviously vanishes. The case $\phi = \phi_{\text{end}}$ is singular because of the first boundary condition of Eq. (2.24), which explains the singularity in Eq. (4.9). The coefficients a_n and b_n can then be expressed as $a_n = \int_{-1}^1 dx P(\mathcal{N} = 0, \phi) \sin[(n+1/2)\pi x]$ for $n \geq 0$ and $b_n = \int_{-1}^1 dx P(\mathcal{N} = 0, \phi) \cos[n\pi x]$ for $n \geq 0$, where we recall that the link between ϕ and x is given above Eq. (4.2). This gives rise to $a_n = 2\pi(n+1/2)/\mu^2$ and $b_n = 0$, hence

$$P(\mathcal{N}, \phi) = \frac{2\pi}{\mu^2} \sum_{n=0}^{\infty} \left(n + \frac{1}{2}\right) \exp\left[-\frac{\pi^2}{\mu^2} \left(n + \frac{1}{2}\right)^2 \mathcal{N}\right] \sin\left[x\pi \left(n + \frac{1}{2}\right)\right], \quad (4.10)$$

which can be written as

$$P(\mathcal{N}, \phi) = -\frac{\pi}{2\mu^2} \vartheta_2' \left(\frac{\pi}{2} x, e^{-\frac{\pi^2}{\mu^2} \mathcal{N}} \right), \quad (4.11)$$

see Eq. (A.4). A few comments are in order.

First, let us stress that the results from both methods, the characteristic function one and the heat equation one, have been necessary to derive this closed form, since the expression coming from the characteristic function has allowed us to calculate the coefficients a_n and b_n in the heat equation solution. This further illustrates how useful it is to have two approaches at hand.

Second, the expansion (4.10) is an alternative to the one given in Eq. (4.3) for the PDF. One can numerically check that they are identical, and in Fig. 5, $P(\mathcal{N}, \phi)$ is displayed as a function of \mathcal{N} for various values of ϕ . The difference between Eqs. (4.3) and (4.10) is that they correspond to expansions around different regions of the PDF. In Eq. (4.3), since one is summing over increasing powers of $e^{-1/\mathcal{N}}$, one is expanding around $\mathcal{N} = 0$, i.e. on the “left” tail of the distribution. In Eq. (4.10) however, since one is summing over increasing powers of $e^{-\mathcal{N}}$, one is expanding around $\mathcal{N} = \infty$, i.e. on the “right” tail of the distribution. Therefore, if one wants to study the PDF by truncating the expansion at some fixed order n , one should choose to work with the expression that better describes the part of the distribution one is interested in, so that both expressions can a priori be useful (let us stress again that, in the limit where all terms in the sums are included, both expressions match exactly for all values of \mathcal{N}).

Third, by plugging $x = 1$ in Eq. (4.11), one obtains an expression for $P(\mathcal{N}, \phi = \phi_{\text{end}} + \Delta\phi_{\text{well}})$ that is an alternative to Eq. (4.4) even if both formulae involve elliptic theta functions. In Appendix A, we show that both expressions are equivalent, due to identities satisfied by the elliptic theta functions. In fact, a third expression for $P(\mathcal{N}, \phi = \phi_{\text{end}} + \Delta\phi_{\text{well}})$ can even be obtained by plugging $x = 1$ into Eq. (4.10) and the consistency with the two other ones is also shown in Appendix A.

Fourth, an approximated formula for the PDF in the limit $\phi \sim \phi_{\text{end}}$ can be derived by Taylor expanding Eq. (4.11),

$$P(\mathcal{N}, \phi \simeq \phi_{\text{end}}) \simeq -\frac{\pi^2}{4\mu^2} x \vartheta_2'' \left(0, e^{-\frac{\pi^2}{\mu^2} \mathcal{N}} \right), \quad (4.12)$$

see Eq. (A.5). This provides an alternative to the approximation (4.5), that is displayed in the right panel of Fig. 6. Numerically, one can check that Eq. (4.5) is slightly better.

Fifth, the PDF of coarse-grained curvature perturbations decays exponentially as $e^{-\zeta_{\text{cg}}}$, i.e. much slower than the Gaussian decay $e^{-\zeta_{\text{cg}}^2}$. Since PBHs form along the tail of these distributions, we expect their mass fraction to be greatly affected by this highly non-Gaussian behaviour. More precisely, on the tail, one has

$$P(\zeta_{\text{cg}}, \phi) \propto e^{-\frac{\pi^2}{4\mu^2} \zeta_{\text{cg}}}, \quad (4.13)$$

which is given by the dominant mode $n = 0$ in the expansion (4.10). Interestingly, the decay rate of the distribution is independent of ϕ . Let us also note that another case

where the PDF decays exponentially is in presence of large local non-Gaussianities, when the PDF is a χ^2 distribution [64, 65].

5 Primordial black holes

The formalism developed so far allows one to derive the PDF of coarse-grained curvature perturbations produced during a phase of single-field slow-roll inflation. Let us now apply this result to the calculation of the mass fraction of PBHs discussed in Sec. 1.

5.1 Classical limit

In the classical limit detailed in Sec. 3, the PDF is approximately Gaussian, see Eq. (3.9), so that the considerations presented in the introduction apply. Plugging Eq. (3.9) into Eq. (1.1), one has $\beta = \text{erfc}[\zeta_c/(2\sqrt{v\gamma_1})]$, which is consistent with Eq. (1.3) as noted below Eq. (3.9). In the $\beta \ll 1$ limit, this leads to

$$v\gamma_1 \simeq -\frac{\zeta_c^2}{4 \ln \beta}, \quad (5.1)$$

where from now on, the order at which the γ_i parameters are calculated is omitted for simplicity. Approximating γ_1 given in Eq. (3.8) by $\gamma_1 \simeq (v/v')^3 \Delta\phi/M_{\text{Pl}}^4$, where $\Delta\phi = |\phi - \phi_{\text{end}}|$ is the field excursion, one obtains

$$\left| \frac{\Delta\phi v^4}{v'^3 M_{\text{Pl}}^4} \right| \simeq -\frac{\zeta_c^2}{4 \ln \beta(M)}. \quad (5.2)$$

In this expression, let us recall that the left-hand side must be evaluated at a value ϕ which is related to the PBH mass M by identifying the wavenumber that exits the Hubble radius during inflation at the time when the inflaton field equals ϕ , with the one that re-enters the Hubble radius during the radiation-dominated era when the mass contained in a Hubble patch equals M . For instance, with $\zeta_c = 1$, the bound $\beta < 10^{-22}$ leads to the requirement that the left-hand side of Eq. (5.2) be smaller than 0.005, which constrains the inflationary potential.

In passing, let us see how the first non-Gaussian correction derived in Sec. 3.1.3 affects this result. Plugging Eq. (3.13) into Eq. (1.1), one obtains

$$\beta(M) = \text{erfc}\left(\frac{\zeta_c}{2\sqrt{v\gamma_1}}\right) + \frac{\gamma_2}{4\sqrt{v\pi}\gamma_1^5} e^{-\frac{\zeta_c^2}{4v\gamma_1}} (\zeta_c^2 - 2v\gamma_1). \quad (5.3)$$

In the $\beta \ll 1$ limit, i.e. in the $\zeta_c^2 \gg v\gamma_1$ limit, this reads $\beta \simeq 2e^{-\zeta_c^2/(4v\gamma_1)} \sqrt{v\gamma_1/\pi}/\zeta_c [1 + \gamma_2 \zeta_c^3/(8v\gamma_1^3)]$. In this regime, one can see that the non-Gaussian correction is in fact larger than the Gaussian leading order, which signals that the non-Gaussian expansion breaks down on the far tail of the distribution. This also suggests that non-Gaussianities cannot be simply treated at the perturbative level when it comes to PBH mass fractions [65].

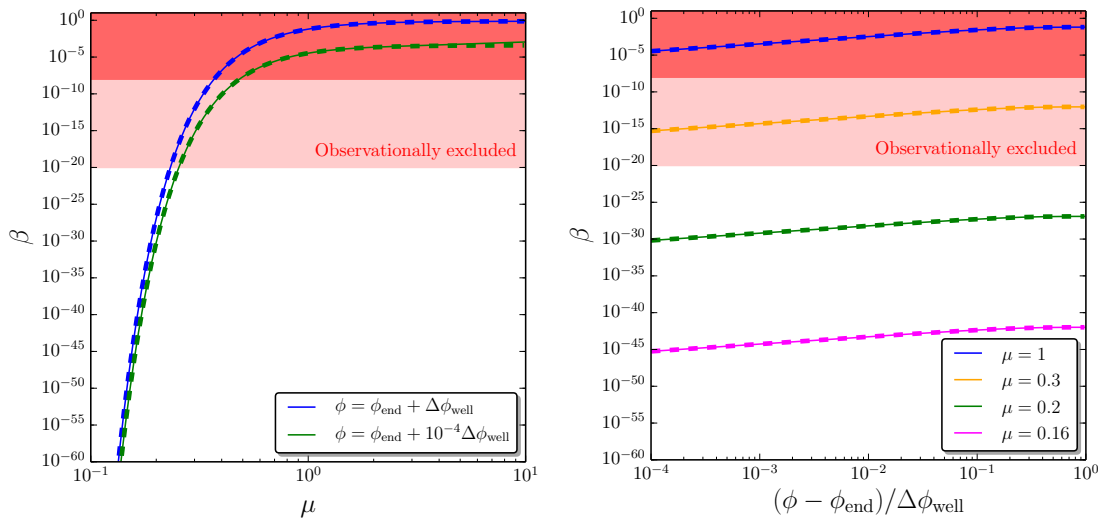


Figure 7. Mass fraction β of primordial black holes in the quantum diffusion dominated regime. The left panel displays β evaluated at $\phi = \phi_{\text{end}} + \Delta\phi_{\text{well}}$ (blue), i.e. at the reflective boundary of the quantum well, and at $\phi = \phi_{\text{end}} + 10^{-4}\Delta\phi_{\text{well}}$, i.e. close to the absorbing boundary of the quantum well, as a function of $\mu = \Delta\phi_{\text{well}}/(\sqrt{v_0}M_{\text{Pl}})$. In the right panel, β is plotted as a function of ϕ for a few values of μ . One can see that the mass fraction depends very weakly on ϕ but very strongly on μ . In both panels, we have taken $\zeta_c = 1$, the solid lines correspond to the full expression (5.4) and the dashed line to the approximation (5.5). The shaded region is excluded by observations, the light shaded area roughly corresponds to constraints for PBH masses between 10^9g and 10^{16}g , the dark shaded area for PBH masses between 10^{16}g and 10^{50}g (see discussion in Sec. 1).

5.2 Stochastic limit

Let us now see how the constraint (5.2) changes in the presence of large quantum diffusion, as considered in Sec. 4. In this case, the PDF of coarse-grained curvature perturbations $\zeta_{\text{cg}} = \delta N_{\text{cg}} = \mathcal{N} - \langle \mathcal{N} \rangle$ can be obtained from Eq. (4.10),

$$\beta(M) = \frac{4}{\pi} \sum_{n=0}^{\infty} \frac{1}{(n + \frac{1}{2})} \sin \left[\pi \left(n + \frac{1}{2} \right) x \right] \exp \left\{ -\pi^2 \left(n + \frac{1}{2} \right)^2 \left[x \left(1 - \frac{x}{2} \right) + \frac{\zeta_c}{\mu^2} \right] \right\}. \quad (5.4)$$

In this expression, we have replaced $\langle \mathcal{N} \rangle = f_1 = \mu^2 x(1 - x/2)$ which can be obtained by setting the potential to a constant in Eq. (2.13). Let us recall that $x = (\phi - \phi_{\text{end}})/\Delta\phi_{\text{well}}$ and that M and ϕ are related as explained below Eq. (5.2). When $x = 0$, i.e. when $\phi = \phi_{\text{end}}$, Eq. (5.4) yields $\beta = 0$, which is consistent with the fact that the PDF of ζ_{cg} is a Dirac distribution in this case.

The mass fraction (5.4) depends only on ϕ , μ and ζ_c . It is displayed in Fig. 7 for $\zeta_c = 1$, as a function of μ for $x = 1$, i.e. $\phi = \phi_{\text{end}} + \Delta\phi_{\text{well}}$, and $x = 10^{-4}$, i.e. $\phi = \phi_{\text{end}} + 10^{-4}\Delta\phi_{\text{well}}$, in the left panel, and as a function of ϕ for a few values of μ in the

right panel. One can see that β depends only weakly on ϕ but very strongly on μ , which is constrained to be at most of order one. More precisely, if one assumes that $\zeta_c \gg \mu^2$ so that ζ_c is well within the tail of the distribution and one can keep only the mode $n = 0$ in Eq. (5.4), as was done when deriving Eq. (4.13), one has

$$\beta(M) \simeq \frac{8}{\pi} \sin\left(\frac{\pi x}{2}\right) e^{-\frac{\pi^2}{8}[x(2-x)] + \frac{2\zeta_c}{\mu^2}}. \quad (5.5)$$

This expression is superimposed to the full result (5.4) in Fig. 7 where one can see that it provides a very good approximation even when the condition $\zeta_c \gg \mu^2$ is not satisfied. This is because, in Eq. (5.4), higher terms in the sum are not only suppressed by higher powers of $e^{-\zeta_c^2/\mu^2}$ but also by higher powers of $e^{-\pi^2 x(1-x/2)}$, so that Eq. (5.5) is an excellent proxy for all values of μ except if x is tiny. With $x = 1$, it gives rise to

$$\mu^2 = \frac{\Delta\phi_{\text{well}}^2}{v_0 M_{\text{Pl}}^2} = -\frac{2\zeta_c}{1 + \frac{8}{\pi^2} \ln\left(\frac{\pi}{8}\beta\right)}. \quad (5.6)$$

Several comments are in order regarding this result. First, with $\zeta_c = 1$, $\beta < 10^{-24}$ gives rise to $\mu < 0.21$ and $\beta < 10^{-5}$ gives rise to $\mu < 0.47$. The requirement that μ be smaller than one is therefore very generic and rather independent of the level of the constraint on β or the precise value chosen for ζ_c . Since v_0 needs to be smaller than 10^{-10} to satisfy the upper bound [14] on the tensor-to-scalar ratio in the CMB observational window, this also means that $\Delta\phi_{\text{well}}$ cannot exceed $\sim 10^{-5} M_{\text{Pl}}$.

Second, Eq. (5.6) should be compared with its classical equivalent, Eq. (5.2). In the left-hand sides of these formulae, the scalings with $\Delta\phi$ and v are not the same. In particular, while the PBH mass fraction increases with the energy scale v in the classical picture, in the stochastic limit, it goes in the opposite direction. One should also note that when the potential is exactly flat, $v' = 0$, the classical result diverges, but the stochastic one remains finite. In the right-hand sides, the scaling with ζ_c is also different, since the shape of the PDF $P(\zeta_{\text{cg}})$ is not the same (it has a Gaussian decay in the classical case and an exponential decay in the stochastic one). The expressions (5.2) and (5.6) are therefore very different, and thus translate into very different constraints on the inflationary potential.

Third, as mentioned below Eq. (5.4), the mean number of e -folds realised across the quantum well is of order μ^2 ,

$$\langle \mathcal{N} \rangle = \mu^2 x \left(1 - \frac{x}{2}\right). \quad (5.7)$$

The conclusion one reaches is therefore remarkably simple: either the region dominated by stochastic effects is much less than one e -fold long and PBHs are not overproduced ($\mu \ll 1$), or it is much more than one e -fold long and PBHs are overproduced ($\mu \gg 1$). Interestingly, heuristic arguments lead to a similar conclusion in Ref. [66], in the context of hybrid inflation.

Fourth, in terms of the power spectrum, since Eq. (2.8) gives $\mathcal{P}_\zeta = f_2'/f_1' - 2f_1$, with f_1 given above and $f_2 = 2\mu^4 x(1 - x^2/2 + x^3/8)/3$ as can be obtained by setting the

potential to a constant in Eq. (2.13), one has

$$\mathcal{P}_\zeta = \frac{2\mu^2}{3} (1-x)^2, \quad (5.8)$$

so μ^2 is also the amplitude of the power spectrum. With $\beta < 10^{-22}$, the constraint (5.6) on μ translates into $\mathcal{P}_\zeta < 1.6 \times 10^{-2}$ for the value of the power spectrum close to the end of inflation. However, contrary to the classical condition $\mathcal{P}_\zeta \Delta N < 10^{-2}$ recalled below Eq. (1.4), this constraint does not involve the number of e -folds since here, a single parameter, μ , determines everything: the mean number of e -folds, the power spectrum amplitude, and the mass fraction.

5.3 Recipe for analysing a generic potential

So far, we have calculated the PBH mass fraction produced in the classical limit and when the inflaton field dynamics are dominated by quantum diffusion. In order to analyse a generic potential, it remains to determine where both limits apply. This can be done by comparing the NLO and NNLO results in the classical limit to estimate the conditions under which the classical expansion is under control. For instance, comparing Eqs. (3.8) and (3.11) for γ_1 , which gives the mass fraction β at NLO as explained in Sec. 5.1, one can see that $|\gamma_1^{\text{NLO}} - \gamma_1^{\text{NNLO}}| \ll \gamma_1^{\text{NLO}}$ if $v \ll 1$ and $|v^2 v''/v'^2| \ll 1$. The first condition is always satisfied, since as already pointed out, v needs to be smaller than 10^{-10} to satisfy the upper bound [14] on the tensor-to-scalar ratio in the CMB observational window. The second condition defines our “classicality criterion” [54]

$$\eta_{\text{class}} \equiv \left| \frac{v^2 v''}{v'^2} \right|. \quad (5.9)$$

When $\eta_{\text{class}} \ll 1$, the classical expansion is under control, at least at NNLO, and one can use the results of Sec. 5.1. Of course, the classical expansion could a priori break down at NNNLO even with $\eta_{\text{class}} \ll 1$, but since higher-order corrections are suppressed by higher powers of v , such a situation is in practice very contrived, and η_{class} provides a rather generic criterion. When $\eta_{\text{class}} \gg 1$, one is far from the classical regime, quantum diffusion dominates the inflaton field dynamics and the results of Sec. 5.2 apply. When η_{class} is of order one, a full numerical treatment is required. The “recipe” for analysing a generic potential is therefore the following:

- calculate η_{class} given by Eq. (5.9) and identify the regions of the potential where $\eta_{\text{class}} \ll 1$ and $\eta_{\text{class}} \gg 1$;
- in the regions where $\eta_{\text{class}} \ll 1$, make use of the constraint from Eq. (5.1);
- in the “quantum wells” defined by $\eta_{\text{class}} \gg 1$, make use of the constraint from Eq. (5.6).

In the following, we illustrate this calculational programme with two examples and check its validity .

5.4 Example 1: $V \propto 1 + \phi^p$

We first consider the case where PBHs can form at scales that exit the Hubble radius towards the end of inflation, where the potential can be approximated by a Taylor expansion around $\phi = 0$ where inflation is assumed to end ($\phi_{\text{end}} = 0$), so

$$v = v_0 \left[1 + \left(\frac{\phi}{\phi_0} \right)^p \right]. \quad (5.10)$$

In this model, inflation does not end by slow-roll violation but another mechanism must be invoked [67–71]. We also assume that the potential is in the vacuum-dominated regime for the range of field values relevant for PBH formation, so that $\phi \ll \phi_0$. A comprehensive study of this potential is performed in Appendix B where all cases of interest are systematically identified and investigated. Here, we simply check that the calculational programme sketched above allows us to recover the main results.

In order to describe the model (5.10) in terms of the situation depicted in Fig. 4, one has to assess $\Delta\phi_{\text{well}}$, which marks the boundary between the classical and the stochastic regimes. In the vacuum-dominated approximation, Eq. (5.9) gives rise to $\eta_{\text{class}} \simeq (p - 1)v_0(\phi/\phi_0)^{-p}/p$, which is of order one when $\phi = \Delta\phi_{\text{well}}$ with

$$\Delta\phi_{\text{well}} \simeq \phi_0 v_0^{\frac{1}{p}}. \quad (5.11)$$

Since $(\Delta\phi_{\text{well}}/\phi_0)^p = v_0 \ll 1$, the vacuum-dominated condition is always satisfied at this transition point. However, the slow-roll conditions are not always met, and in Appendix B it is shown that slow roll is indeed violated at $\phi = \Delta\phi_{\text{well}}$ if $\phi_0/M_{\text{Pl}} < v_0^{(p-2)/(2p)}$, unless $p = 1$ for which slow-roll is violated if $\phi_0 < M_{\text{Pl}}$. In such cases, the expansion (5.10) fails to cover the whole quantum well and higher-order terms in the potential must be included for a consistent analysis. Otherwise, we can keep following the recipe given above.

In the classical regime, $\phi \gg \Delta\phi_{\text{well}}$, Eq. (5.1) applies, where $v\gamma_1$ is given by Eq. (3.8). In the vacuum-dominated approximation, it reads $v\gamma_1 \simeq v_0(\phi_0/M_{\text{Pl}})^4/(4p^3 - 3p^4)[(\phi/\phi_0)^{4-3p} - (\phi_{\text{end}}/\phi_0)^{4-3p}]$. Neglecting the contribution from ϕ_{end} , which lies outside the validity range of the classical formula anyway, one can evaluate this expression at $\phi = \Delta\phi_{\text{well}}$ where the power spectrum is maximal, and combining this with Eq. (5.1) leads to

$$\frac{v_0^{\frac{2}{p}-1}}{\sqrt{|4p^3 - 3p^4|}} \left(\frac{\phi_0}{M_{\text{Pl}}} \right)^2 \simeq \frac{\zeta_{\text{c}}}{2\sqrt{|\ln \beta|}}. \quad (5.12)$$

In the stochastic regime, combining Eqs. (5.6) and (5.11), one has

$$v_0^{\frac{2}{p}-1} \left(\frac{\phi_0}{M_{\text{Pl}}} \right)^2 \simeq \frac{2\zeta_{\text{c}}}{\left| 1 + \frac{8}{\pi^2} \ln \left(\frac{\pi}{8} \beta \right) \right|}. \quad (5.13)$$

It is interesting to notice that up to an overall factor of order one, the two constraints (5.12) and (5.13) are very similar, even though they are obtained in very different regimes that yield very different PDFs for the curvature perturbations.

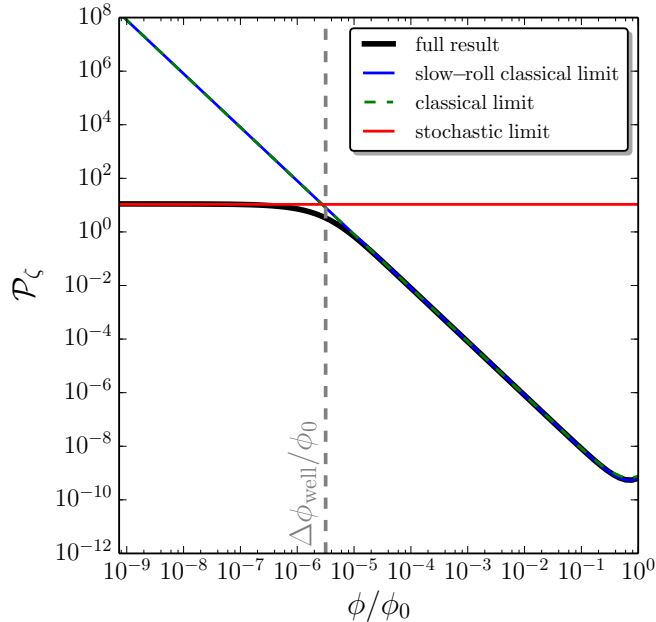


Figure 8. Power spectrum of curvature perturbations \mathcal{P}_ζ produced in the potential (5.10) with $p = 2$, $v_0 = 10^{-11}$, $\phi_0 = 4M_{\text{Pl}}$ and $\phi_{\text{uv}} = 10^4\phi_0$ (solid black line). The blue line corresponds to the slow-roll classical limit (1.5), while the green dashed line is obtained from solving the full Klein-Gordon equation. The red line corresponds to the stochastic limit assuming the potential is exactly flat for $\phi < \Delta\phi_{\text{well}}$ and that a reflective wall is located at $\phi = \Delta\phi_{\text{well}}$. The value of $\Delta\phi_{\text{well}}$ obtained from requiring $\eta_{\text{class}} = 1$ is displayed with the grey vertical dotted line and delimitates the classical and stochastic regimes.

It is also important to note that the slow-roll conditions given above imply that $v_0^{2/p-1}(\phi_0/M_{\text{Pl}})^2 \gg 1$ except if $p = 1$. Therefore, if p is different from 1, either PBHs are too abundant and the model is ruled out, or slow roll is strongly violated before one exits the classical regime and one needs to go beyond the present formalism to calculate PBH mass fractions. The case $p = 1$ is subtle, since Eq. (5.9) gives $\eta_{\text{class}} = 0$. One would thus have to extend the classical expansion of Sec. 3 to next-to-next-to-next to leading order (NNNLO) to determine what the first stochastic correction is and under which condition the classical approximation holds, and investigate numerically the regime where it does not. This goes beyond the scope of the present paper and we leave this study for future work.

In passing, let us check that approximating the full potential (5.10) as a piecewise function consisting of a constant piece and a classical one, separated at $\phi = \Delta\phi_{\text{well}}$, is numerically justified. In Fig. 8, we show the power spectrum computed numerically from Eqs. (2.13) and (2.8), which gives $\mathcal{P}_\zeta = f'_2/f'_1 - 2f_1$, in the potential (5.10) with $p = 2$, $v_0 = 10^{-11}$, $\phi_0 = 4M_{\text{Pl}}$ and $\phi_{\text{uv}} = 10^4\phi_0$ (solid black line). The blue line corresponds to the slow-roll classical limit (1.5), and the green dashed line is obtained

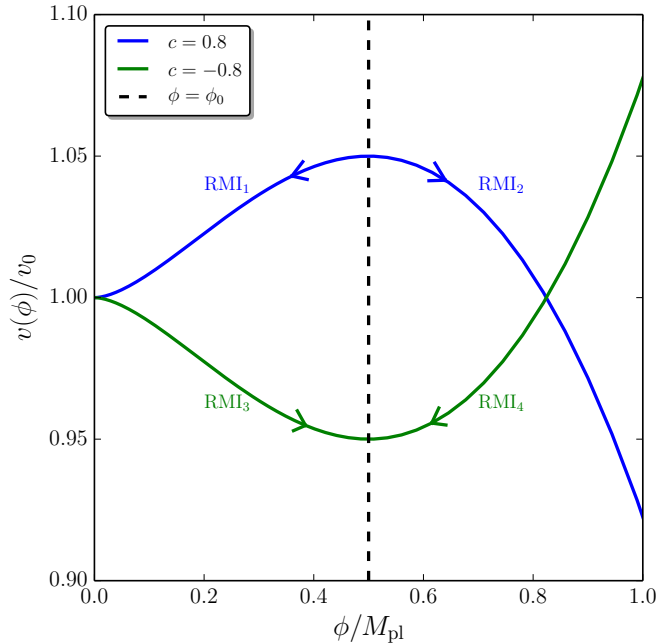


Figure 9. The potential (5.14) for running-mass inflation (RMI) with $\phi_0 = 0.5M_{\text{Pl}}$. The blue curve takes $c = 0.8$ and the green curve takes $c = -0.8$ (these values may not be physical but they have been chosen to produce a clear plot). RMI is shown to have four possible realisations (RMI₁, RMI₂, RMI₃ and RMI₄), depending on the sign of c and on whether ϕ is initially smaller or larger than ϕ_0 . Except for RMI₂, the potential flattens as inflation proceeds, which can lead to the formation of PBHs for scales exiting the Hubble radius towards the end of inflation.

from solving the full Klein-Gordon equation. The agreement of this solution with the slow-roll formula confirms that the slow-roll conditions are satisfied for the parameters used in this example. The red line corresponds to the stochastic limit (5.8) $\mathcal{P}_\zeta = 2\mu^2/3$ at $\phi = 0$, where μ is given by Eqs. (4.2) and (5.11), which yields $\mathcal{P}_\zeta \sim 2(\phi_0/M_{\text{Pl}})^2 v_0^{2/p-1}/3$. One can see that both limits are correctly reproduced, and that the value of $\Delta\phi_{\text{well}}$ obtained in Eq. (5.11) from our classicality criterion $\eta_{\text{class}} < 1$, and displayed with the grey vertical dotted line, indeed separates the two regimes. In Appendix B, an analytical expression for \mathcal{P}_ζ in the regime $\phi \ll \Delta\phi_{\text{well}}$ is derived, and one finds $\mathcal{P}_\zeta = 2\Gamma^2(1/p)v_0^{2/p-1}(\phi_0/M_{\text{Pl}})^2/p^2$, see Eq. (B.11), where Γ is the gamma function. Up to an overall numerical constant of order one, one recovers the result obtained from simply assuming the potential to be exactly flat until $\phi = \Delta\phi_{\text{well}}$, where $\eta_{\text{class}} = 1$, and setting a reflective wall there. This confirms the validity of this approach.

5.5 Example 2: running-mass inflation

Let us now consider another example, running-mass inflation (RMI) [72], where the inflationary potential is given by

$$v(\phi) = v_0 \left\{ 1 - \frac{c}{2} \left[-\frac{1}{2} + \ln \left(\frac{\phi}{\phi_0} \right) \right] \frac{\phi^2}{M_{\text{Pl}}^2} \right\}. \quad (5.14)$$

In this expression, c is a dimensionless coupling constant assumed to be much smaller than one, $c \ll 1$ (more precisely, as discussed in Ref. [73], within supersymmetry, natural values of c are $c \simeq 10^{-2}$ to 10^{-1} for soft masses values matching the energy scale of inflation), and ϕ_0 must be sub-Planckian, $\phi_0 \ll M_{\text{Pl}}$.

The potential (5.14) is displayed in Fig. 9, where one can see that depending on the sign of c and on whether ϕ is initially smaller or larger than ϕ_0 , inflation can proceed in four regimes [74], that we denote RMI₁, RMI₂, RMI₃ and RMI₄. In RMI₁, $c > 0$, $\phi < \phi_0$ and ϕ decreases towards $\phi = 0$ as inflation proceeds. RMI₂ also has $c > 0$ but in this case $\phi > \phi_0$ and ϕ increases away from ϕ_0 throughout inflation. RMI₃ and RMI₄ both have $c < 0$, but RMI₃ has $\phi < \phi_0$ with ϕ increasing towards ϕ_0 during inflation, while RMI₄ has $\phi > \phi_0$ and ϕ decreases towards ϕ_0 during inflation. In RMI₁, RMI₃ and RMI₄, the potential flattens as inflation proceeds, which may lead to the production of PBHs at scales that exit the Hubble radius towards the end of inflation, as studied in Refs. [75–77]. The width of the “quantum well” in these cases is determined by the condition $\eta_{\text{class}} > 1$, where η_{class} is given by Eq. (5.9). In the vacuum-dominated regime, it reads

$$\eta_{\text{class}} \simeq \frac{v_0}{|c|} \frac{M_{\text{Pl}}^2}{\phi^2} \frac{\left| 1 + \ln \left(\frac{\phi}{\phi_0} \right) \right|}{\ln^2 \left(\frac{\phi}{\phi_0} \right)}. \quad (5.15)$$

For RMI₁, the equation $\eta_{\text{class}}(\phi_{\text{well}}) = 1$ yields $\phi_{\text{well}}/\phi_0 \sqrt{|\ln(\phi_{\text{well}}/\phi_0)|} = \sqrt{v_0/c} M_{\text{Pl}}/\phi_0$, where we have assumed that $\phi_{\text{well}} \ll \phi_0$ so that $|\ln(\phi_{\text{well}}/\phi_0)| \gg 1$. This can be solved as

$$\phi_{\text{well}} = \phi_0 \exp \left[\frac{1}{2} W_{-1} \left(-2 \frac{v_0}{c} \frac{M_{\text{Pl}}^2}{\phi_0^2} \right) \right], \quad (5.16)$$

where W_{-1} is the -1 branch of the Lambert function [78]. The approximation $|\ln(\phi_{\text{well}}/\phi_0)| \gg 1$ is satisfied when the argument of the Lambert function in Eq. (5.16) is much smaller than one, which is typically the case for the values of v_0 , c and ϕ_0 considered in the literature [73, 79]. In this limit, one can Taylor expand the Lambert function according to $W_{-1}(-x) \simeq \ln x$ when $x \ll 1$, which gives rise to $\phi_{\text{well}} \simeq \sqrt{2v_0/c} M_{\text{Pl}}$, and hence

$$\Delta\phi_{\text{well}} = |\phi_{\text{well}}| \simeq \sqrt{\frac{2v_0}{c}} M_{\text{Pl}}. \quad (5.17)$$

In this expression, we have assumed that inflation terminates at $\phi = 0$ (otherwise, ϕ_{end} must be subtracted from the right-hand side). Making use of Eq. (4.2), this leads to

$$\mu^2 \simeq \frac{2}{c} \gg 1. \quad (5.18)$$

The result is remarkably simple since it depends only on the coupling constant c , and on neither v_0 nor ϕ_0 . As explained at the beginning of this section, c is always much smaller than one, which implies that $\mu \gg 1$ and according to the discussion of Sec. 5.2, PBHs are too abundant in this case. One concludes that the stochastic regime of the potential cannot be explored in RMI₁, i.e. ϕ_{end} should be at least of the order of $\Delta\phi_{\text{well}}$ given in Eq. (5.17).

For RMI₂, the potential does not flatten as inflation proceeds so the inflaton field dynamics is never dominated by quantum diffusion for scales smaller than those probed in the CMB.

For RMI₃ and RMI₄, assuming that ϕ_{well} is very close to ϕ_0 so that $|\ln(\phi_{\text{well}}/\phi_0)| \ll 1$, the equation $\eta_{\text{class}}(\phi_{\text{well}}) = 1$ reduces to $\phi_{\text{well}}/\phi_0 |\ln(\phi_{\text{well}}/\phi_0)| = \sqrt{v_0/|c|} M_{\text{Pl}}/\phi_0$. This can be solved as

$$\phi_{\text{well}} = \phi_0 \exp \left[W_0 \left(\mp \sqrt{\frac{v_0}{|c|}} \frac{M_{\text{Pl}}}{\phi_0} \right) \right], \quad (5.19)$$

where W_0 is the principal branch of the Lambert function, and its argument comes with a minus sign in RMI₃ and with a plus sign in RMI₄. The approximation $|\ln(\phi_{\text{well}}/\phi_0)| \ll 1$ is satisfied when the argument of the Lambert function in Eq. (5.19) is much smaller than one, which is the same condition as the one coming from $\phi_{\text{well}} \ll \phi_0$ in RMI₁. In this limit, one can Taylor expand the Lambert function as $W_0(x) \simeq x$ when $x \ll 1$. One obtains $\phi_{\text{well}} \simeq \phi_0 \mp M_{\text{Pl}} \sqrt{v_0/|c|}$, and hence

$$\Delta\phi_{\text{well}} = |\phi_{\text{well}} - \phi_0| \simeq M_{\text{Pl}} \sqrt{\frac{v_0}{|c|}}. \quad (5.20)$$

Up to a factor $\sqrt{2}$, this expression is the same as Eq. (5.17). This leads to

$$\mu^2 \simeq \frac{1}{|c|} \gg 1, \quad (5.21)$$

and the same conclusions as the ones drawn for RMI₁ apply, namely that one cannot explore the quantum well of the potential without producing too many PBHs, so $|\phi_{\text{end}} - \phi_0|$ should be at least of order $\Delta\phi_{\text{well}}$ given in Eq. (5.20).

If this is indeed the case, the classical approximation is valid throughout the entire period of inflation, and Eq. (1.5) gives rise to

$$\mathcal{P}_\zeta \simeq 2 \frac{v_0}{c^2} \frac{M_{\text{Pl}}^2}{\phi^2} \ln^{-2} \left(\frac{\phi}{\phi_0} \right). \quad (5.22)$$

When this expression is evaluated at ϕ_{well} , given by Eq. (5.16) for RMI₁ and by Eq. (5.19) for RMI₃ and RMI₄, one finds

$$\mathcal{P}_\zeta(\phi_{\text{well}}) \simeq \begin{cases} \frac{4}{c} & \text{in RMI}_1 \\ \frac{2}{|c|} & \text{in RMI}_3 \text{ and RMI}_4 \end{cases}. \quad (5.23)$$

It is interesting to notice that, up to an overall numerical constant of order one, this also corresponds to the stochastic limit (5.8), $\mathcal{P}_\zeta \sim \mu^2 \sim 1/c$, where one makes use of

Eqs. (5.18) and (5.21). This is similar to what was found in Sec. 5.4. Since $|c| \ll 1$, this means that the classical power spectrum is already larger than one when one enters the quantum well. This implies that, for this model, analyses relying on the classical formalism only should exclude the quantum well (even if not for the correct reason) and should therefore be valid. Let us however stress that the approach developed in this work was necessary in order to check the consistency of the standard results.

6 Conclusion

Let us now summarise our main findings. Making use of the stochastic- δN formalism, we have developed a calculational framework in which the PDF of the coarse-grained curvature perturbations produced during inflation can be derived exactly, even in the presence of large quantum backreaction on the inflaton field dynamics. More precisely, we have proposed two complementary methods, one based on solving an ordinary differential equation for the characteristic function of the PDF, and the other based on solving a heat equation for the PDF directly. We have shown that depending on the problem one considers, the method to be preferred can vary. We have then derived a classicality criterion that determines whether the effects of quantum diffusion are important or not. When this is not the case, i.e. in the classical limit, we have developed an expansion scheme that not only recovers the standard Gaussian PDF at leading order, but also allows one to calculate the first non-Gaussian corrections to the usual result. In the opposite limit, i.e. when quantum diffusion plays the dominant role in the field dynamics, we have found that the PDF follows an elliptic theta function, whose tail decays only exponentially, and which is fully characterised by a single parameter, given by $\mu^2 = \Delta\phi_{\text{well}}^2/(v_0 M_{\text{Pl}}^2)$. This parameter measures the ratio between the squared width of the quantum well and its height, in Planck mass units. The mean number of e -folds realised across the quantum well, the amplitude of the power spectrum, and, if $\zeta_c \sim 1$, the inverse log of the PBH mass fraction, are all of order μ^2 . Therefore, observational constraints on the abundance of PBHs put an upper bound on μ^2 that is of order one, and imposes that one cannot spend more than ~ 1 e -fold in regions of the potential dominated by quantum diffusion. For a given potential, one must therefore determine whether a diffusion dominated quantum well exists, and check that its width squared is smaller than its height. Finally, we have illustrated our calculational programme with two examples.

We now mention a few of the new and interesting research directions that open up as a consequence of the results obtained in this work:

- First, we have shown that the effects of quantum diffusion on the PDF of curvature perturbations and on the mass fraction of PBHs can be dramatic in regions of the potential where the classical approximation breaks down. This implies that some of the constraints on inflationary models derived in the literature, from non-observations of PBHs and using only the classical approximation, may have to be revised. This could have important consequences for these models.

- Second, we have seen that even when the classical approximation is under control close to the maximum of the PDF, it fails on its tail, where deviations from Gaussianity cannot be simply described by increasing the order at which the classical expansion is performed. Since PBHs are precisely sourced by the tail of the distribution of curvature perturbations, this implies that a more thorough investigation of quantum diffusion effects on PBH mass fraction may be required, even in what is referred to as the “classical” regime in the present work.
- Third, there are cases where slow roll is violated when scales smaller than those probed in the CMB exit the Hubble radius and the standard PBH calculation does not apply, as recently pointed out in Refs. [80–82]. This, for instance, happens when the inflationary potential has a flat inflection point [83], around which slow roll is transiently violated and one can even enter an ultra slow-roll phase. However, close to the inflection point, quantum diffusion plays an important role and this also needs to be included. This requires the formalism presented in this work to be extended beyond the slow-roll approximation [84].
- Fourth, it has recently been shown [56, 57] that in presence of multiple fields, the effects of quantum diffusion can be even more drastic. Formation of PBHs in multi-field models of inflation, such as hybrid inflation [55, 66, 85–87], would therefore be interesting to study with our formalism.
- Fifth and finally, there are other astrophysical objects for which the knowledge of the full probability distribution of cosmological perturbations produced during inflation is important, such as ultra-compact mini-halos [88]. Using our results to calculate the abundance of such objects is also an interesting prospect.

Acknowledgments

It is a pleasure to thank Chris Byrnes and Sam Young for enjoyable discussions and useful comments. V.V. acknowledges funding from the European Union’s Horizon 2020 research and innovation programme under the Marie Skłodowska-Curie grant agreement N^o 750491. V.V., H.A. and D.W. acknowledge financial support from STFC grant ST/N000668/1.

A Elliptic theta functions

In Sec. 4, the PDF of coarse-grained curvature perturbations is expressed in terms of elliptic theta functions. In this appendix, we define these special functions and give some of their properties that are relevant for the considerations of Sec. 4. There are four

elliptic theta functions, defined as [62, 63]

$$\begin{aligned}
\vartheta_1(z, q) &= 2 \sum_{n=0}^{\infty} (-1)^n q^{(n+\frac{1}{2})^2} \sin [(2n+1)z] , \\
\vartheta_2(z, q) &= 2 \sum_{n=0}^{\infty} q^{(n+\frac{1}{2})^2} \cos [(2n+1)z] , \\
\vartheta_3(z, q) &= 1 + 2 \sum_{n=1}^{\infty} q^{n^2} \cos (2nz) , \\
\vartheta_4(z, q) &= 1 + 2 \sum_{n=1}^{\infty} (-1)^n q^{n^2} \cos (2nz) .
\end{aligned} \tag{A.1}$$

By convention, ϑ'_i denotes the derivative of ϑ_i with respect to its first argument z . For instance, one has

$$\vartheta'_1(z, q) = 2 \sum_{n=0}^{\infty} (-1)^n q^{(n+\frac{1}{2})^2} (2n+1) \cos [(2n+1)z] , \tag{A.2}$$

which appears in Eq. (4.4). As another example, one has

$$\vartheta''_4(z, q) = -8 \sum_{n=1}^{\infty} (-1)^n q^{n^2} n^2 \cos (2nz) , \tag{A.3}$$

which is used in Eq. (4.5). As a third example, one has

$$\vartheta'_2(z, q) = -2 \sum_{n=0}^{\infty} q^{(n+\frac{1}{2})^2} (2n+1) \sin [(2n+1)z] , \tag{A.4}$$

which appears in Eq. (4.11). As a last example, one has

$$\vartheta''_2(z, q) = -2 \sum_{n=0}^{\infty} q^{(n+\frac{1}{2})^2} (2n+1)^2 \cos [(2n+1)z] , \tag{A.5}$$

which is used in Eq. (4.12). The function $\vartheta_i(z, q)$ is noted `EllipticTheta[i, z, q]` in Mathematica and $\vartheta'_i(z, q)$ is noted `EllipticThetaPrime[i, z, q]`.

Let us now show that the different expressions for $P(\mathcal{N}, \phi = \phi_{\text{end}} + \Delta\phi_{\text{well}})$ obtained in Sec. 4 in the stochastic dominated regime are equivalent. A first expression is given by Eq. (4.4), a second expression can be derived by plugging $x = 1$ into Eq. (4.10) and making use of Eq. (A.2), and a third expression is given by plugging $x = 1$ in Eq. (4.11). The three formulae are equivalent if

$$\left(\frac{\mu}{\sqrt{\pi\mathcal{N}}} \right)^3 \vartheta'_1 \left(0, e^{-\frac{\mu^2}{\mathcal{N}}} \right) = \vartheta'_1 \left(0, e^{-\frac{\pi^2}{\mu^2}\mathcal{N}} \right) = -\vartheta'_2 \left(\frac{\pi}{2}, e^{-\frac{\pi^2}{\mu^2}\mathcal{N}} \right) . \tag{A.6}$$

The first equality in Eq. (A.6) can be shown from the Jacobi identity for a modular transformation of the first elliptic theta function, see Eq. (20.7.30) of Ref. [89],

$$(-i\tau)^{\frac{1}{2}} \vartheta_1(z, e^{i\pi\tau}) = -ie^{-\frac{z^2}{\pi\tau}} \vartheta_1\left(-\frac{z}{\tau}, -e^{-\frac{i\pi}{\tau}}\right). \quad (\text{A.7})$$

By taking $\tau = i/(a\pi)$ and differentiating Eq. (A.7) with respect to z , one obtains

$$(\pi a)^{\frac{1}{2}} \vartheta_1'(z, e^{-\frac{1}{a}}) = -\frac{2iz}{a} e^{az^2} \vartheta_1(-i\pi az, e^{-\pi^2 a}) + a\pi e^{az^2} \vartheta_1'(-i\pi az, e^{-\pi^2 a}). \quad (\text{A.8})$$

Taking $z = 0$, one recovers the first equality in Eq. (A.6). The second equality in Eq. (A.6) simply follows from Eqs. (A.2) and (A.4).

B Detailed analysis of the model $V \propto 1 + \phi^p$

In this appendix, we present a detailed analysis of the model discussed in Sec. 5.4, where the inflationary potential is of the form

$$v(\phi) = v_0 \left[1 + \left(\frac{\phi}{\phi_0} \right)^p \right]. \quad (\text{B.1})$$

In order to use the slow-roll approximation, one needs to check that the slow-roll conditions [90], $M_{\text{Pl}}^2 (v'/v)^2 \ll 1$, $M_{\text{Pl}}^2 |v''/v| \ll 1$, and $M_{\text{Pl}}^4 |v'''v'/v^2| \ll 1$, are satisfied. Here, we use the three first slow-roll conditions only, since these are the only ones currently constrained by observations. In order to satisfy the third condition, one requires a condition involving the position of ϕ with respect to

$$\phi_{\text{sr1}} \equiv \phi_0 \left(\frac{\phi_0}{M_{\text{Pl}}} \right)^{\frac{2}{p-2}}, \quad (\text{B.2})$$

i.e. $\phi \ll \phi_{\text{sr1}}$ if $p > 2$ and $\phi \gg \phi_{\text{sr1}}$ if $p < 2$. The second slow-roll condition reduces to an equivalent condition. If $p = 1$, there is no such condition and if $p = 2$, it reduces to $\phi_0 \gg M_{\text{Pl}}$. The first condition constrains the position of ϕ with respect to

$$\phi_{\text{sr2}} \equiv \phi_0 \left(\frac{\phi_0}{M_{\text{Pl}}} \right)^{\frac{1}{p-1}}, \quad (\text{B.3})$$

namely $\phi \ll \phi_{\text{sr2}}$ if $p > 1$ and $\phi \gg \phi_{\text{sr2}}$ if $p < 1$ (if $p = 1$, it reduces to $\phi_0 \gg M_{\text{Pl}}$).

As explained in Sec. 5.4, quantum diffusion plays an important role when $\eta_{\text{class}} \gg 1$, where η_{class} is given in Eq. (5.9), which leads to $\phi \ll \Delta\phi_{\text{well}}$, where

$$\Delta\phi_{\text{well}} = \phi_0 v_0^{\frac{1}{p}}, \quad (\text{B.4})$$

see Eq. (5.11). Hereafter, we work in the vacuum-dominated regime, in which $\phi \ll \phi_0$ and $v \simeq v_0$. Making use of Eq. (5.6), this gives rise to

$$\mu^2 = \left(\frac{\phi_0}{M_{\text{Pl}}} \right)^2 v_0^{\frac{2}{p}-1}. \quad (\text{B.5})$$

In the classical regime, i.e. when $\phi \gg \Delta\phi_{\text{well}}$, the power spectrum is given by Eq. (1.5), which gives rise to

$$\mathcal{P}_\zeta|_{\text{cl}} = \frac{2v_0}{p^2} \left(\frac{\phi_0}{M_{\text{Pl}}} \right)^2 \left(\frac{\phi_0}{\phi} \right)^{2p-2}. \quad (\text{B.6})$$

Thus we see that the classical power spectrum is larger than unity when $\phi < \phi_{\mathcal{P}_\zeta|_{\text{cl}} > 1}$ if $p > 1$, and $\phi > \phi_{\mathcal{P}_\zeta|_{\text{cl}} > 1}$ if $p < 1$, where

$$\phi_{\mathcal{P}_\zeta|_{\text{cl}} > 1} = \phi_0 \left[\frac{2v_0}{p^2} \left(\frac{\phi_0}{M_{\text{Pl}}} \right)^2 \right]^{\frac{1}{2p-2}}. \quad (\text{B.7})$$

The number of e -folds realised between ϕ and ϕ_{end} can also be calculated in the classical regime using Eq. (1.5), and one obtains

$$N_{\text{end}} - N \simeq \frac{\phi_0^2}{p(p-2)M_{\text{Pl}}^2} \left[\left(\frac{\phi_0}{\phi_{\text{end}}} \right)^{p-2} - \left(\frac{\phi_0}{\phi} \right)^{p-2} \right]. \quad (\text{B.8})$$

Note that this expression is singular for $p = 2$, and this case is treated separately in Sec. B.1. Combining Eqs. (B.7) and (B.8), one can rewrite the classical power spectrum as

$$\mathcal{P}_\zeta|_{\text{cl}} = \frac{2v_0}{p^2} \left(\frac{\phi_0}{M_{\text{Pl}}} \right)^2 \left[\frac{p(2-p)M_{\text{Pl}}^2}{\phi_0^2} (N_{\text{end}} - N) + \left(\frac{\phi_0}{\phi_{\text{end}}} \right)^{p-2} \right]^{\frac{2p-2}{p-2}}. \quad (\text{B.9})$$

In the stochastic regime, i.e. when $\phi \ll \Delta\phi_{\text{well}}$, the mean number of e -folds can be computed from Eq. (2.13) for f_1 . In the limit $\phi_{\text{uv}} \rightarrow \infty$, and taking $\phi \ll \Delta\phi_{\text{well}}$, one obtains

$$\langle \mathcal{N} \rangle = \Gamma \left(\frac{1}{p} \right) \frac{\phi_0}{pM_{\text{Pl}}^2 v_0^{1-\frac{1}{p}}} (\phi - \phi_{\text{end}}). \quad (\text{B.10})$$

Similarly, using Eq. (2.13) for f_2 , and the formula $\mathcal{P}_\zeta = f_2'/f_1' - 2f_1$ from Eq. (2.8), the power spectrum is given by

$$\mathcal{P}_\zeta(\phi) = \frac{2}{p^2} \Gamma^2 \left(\frac{1}{p} \right) v_0^{\frac{2}{p}-1} \left(\frac{\phi_0}{M_{\text{Pl}}} \right)^2. \quad (\text{B.11})$$

B.1 Case $p = 2$

We first consider the case of $p = 2$, where the slow-roll conditions reduce to $\phi_0 \gg M_{\text{Pl}}$. Let us also note that Eq. (B.8) is singular for $p = 2$, and that it should be replaced by

$$N_{\text{end}} - N \simeq \frac{\phi_0^2}{2M_{\text{Pl}}^2} \ln \left(\frac{\phi_0}{\phi_{\text{end}}} \right). \quad (\text{B.12})$$

As noted in Sec. 5.4, the constant value found for the power spectrum in the stochastic limit, Eq. (B.11), corresponds (up to an order one prefactor) to the classical power

spectrum (B.9) evaluated at $\Delta\phi_{\text{well}}$. Therefore, when ϕ decreases, the stochastic and the classical result coincide until ϕ becomes smaller than $\Delta\phi_{\text{well}}$, where the stochastic power spectrum saturates to a constant value and the classical power spectrum continues to increase. Since the slow-roll condition implies that $\phi_0 \gg M_{\text{Pl}}$, the power spectrum is always larger than one in this regime. This can be also seen from $\phi_{\mathcal{P}_\zeta|_{\text{cl}} > 1} < \Delta\phi_{\text{well}}$, as can be checked explicitly from Eqs. (B.4) and (B.7).

Furthermore, the number of e -folds (B.10) spent in the stochastic regime is of order $\langle \mathcal{N} \rangle = \sqrt{\pi}/2(\phi_0/M_{\text{Pl}})^2$, which is larger than unity. It is interesting to note that both the amplitude of the power spectrum and the number of e -folds during which the stochastic regime depend only on ϕ_0 . PBHs are therefore overproduced in this case.

B.2 Case $p > 2$

We now consider values of p such that $p > 2$. In this case, the slow-roll condition that is the strictest depends on whether ϕ_0 is sub-Planckian or super-Planckian. More precisely, since $2/(p-2) > 1/(p-1)$ for $p > 2$, if $\phi_0 < M_{\text{Pl}}$, then $\phi_{\text{sr1}} < \phi_{\text{sr2}}$ and the slow-roll condition is given by $\phi \ll \phi_{\text{sr1}}$, and if $\phi_0 > M_{\text{Pl}}$ then $\phi_{\text{sr2}} < \phi_{\text{sr1}}$ and it is given by $\phi \ll \phi_{\text{sr2}}$.

B.2.1 Case $p > 2$ and $\phi_0 > M_{\text{Pl}}$

In this case, the slow-roll condition reads $\phi \ll \phi_{\text{sr2}}$. Making use of Eqs. (B.3), (B.4) and (B.7), one can show that

$$\Delta\phi_{\text{well}} < \phi_{\mathcal{P}_\zeta|_{\text{cl}} > 1} < \phi_{\text{sr2}}. \quad (\text{B.13})$$

As a consequence, when stochastic effects become important, the classical power spectrum is already larger than one and so quantum diffusion cannot “rescue” the model in this case. Stochastic effects do reduce the amount of power, but not soon enough to keep the amount of PBH below the observationally constrained level.

B.2.2 Case $p > 2$ and $\phi_0 < M_{\text{Pl}}$

In this case, the slow-roll condition reads $\phi \ll \phi_{\text{sr1}}$. Two sub-cases need to be distinguished.

Case $p > 2$ and $v_0^{\frac{p-2}{2p}} < \phi_0/M_{\text{Pl}} < 1$

In this case, Eqs. (B.2), (B.4) and (B.7) lead to

$$\Delta\phi_{\text{well}} < \phi_{\mathcal{P}_\zeta|_{\text{cl}} > 1} < \phi_{\text{sr1}}. \quad (\text{B.14})$$

The situation is therefore very similar to the case $p > 2$ and $\phi_0 > M_{\text{Pl}}$, and quantum diffusion does not sufficiently suppress PBH production.

Case $p > 2$ and $\phi_0/M_{\text{Pl}} < v_0^{\frac{p-2}{2p}}$

In this case, Eqs. (B.2), (B.4) and (B.7) give a reversed hierarchy, namely

$$\phi_{\text{sr1}} < \phi_{\mathcal{P}_\zeta|_{\text{cl}} > 1} < \Delta\phi_{\text{well}}. \quad (\text{B.15})$$

In the region where the slow-roll approximation applies, $\phi \ll \phi_{\text{sr1}}$, the classical power spectrum is therefore always larger than one. However this region is dominated by stochastic effects since $\phi_{\text{sr1}} < \Delta\phi_{\text{well}}$. In the stochastic regime, the expressions we have previously derived receive a contribution from $\phi > \phi_{\text{sr1}}$ since we are integrating beyond $\Delta\phi_{\text{well}}$, and are therefore inconsistent in this case. Intuitively, one may think that the violation of slow roll induces the suppression of the noise amplitude in the Langevin equation (1.6) so that $\Delta\phi_{\text{well}}$ should in fact be replaced with ϕ_{sr1} . The situation is then similar to the one sketched in Fig. 4, and from Eqs. (4.2) and (B.2), one has

$$\mu^2 \sim \frac{\phi_{\text{sr1}}^2}{v_0 M_{\text{Pl}}^2} = \frac{1}{v_0} \left(\frac{\phi_0}{M_{\text{Pl}}} \right)^{\frac{2p}{p-2}}. \quad (\text{B.16})$$

Since the condition under which this case is defined is $\phi_0/M_{\text{Pl}} < v_0^{\frac{p-2}{2p}}$, one has $\mu^2 < 1$, and PBHs are not overproduced in this case.

B.3 Case $1 < p < 2$

In this case, slow roll is valid in the range

$$\phi_{\text{sr1}} \ll \phi \ll \phi_{\text{sr2}}. \quad (\text{B.17})$$

Note that this condition implies that $\phi_{\text{sr1}} \ll \phi_{\text{sr2}}$, which is the case only if $\phi_0 \gg M_{\text{Pl}}$. One then has $\phi_{\text{sr2}} \gg \phi_0$, so this range extends beyond the vacuum-dominated regime, and the interval of interest is in fact

$$\phi_{\text{sr1}} \ll \phi \ll \phi_0. \quad (\text{B.18})$$

Two sub-cases need to be distinguished.

B.3.1 Case $1 < p < 2$ and $\phi_0/M_{\text{Pl}} < v_0^{\frac{p-2}{2p}}$

In this case, Eqs. (B.2), (B.3), (B.4) and (B.7) give rise to

$$\phi_{\mathcal{P}_\zeta|_{\text{cl}} > 1} < \Delta\phi_{\text{well}} < \phi_{\text{sr1}} < \phi_0 < \phi_{\text{sr2}}. \quad (\text{B.19})$$

This means that in the region of interest given by Eq. (B.18), the classical approximation is valid and predicts that PBHs are not overproduced.

B.3.2 Case $1 < p < 2$ and $\phi_0/M_{\text{Pl}} > v_0^{\frac{p-2}{2p}}$

In this case, Eqs. (B.2), (B.3), (B.4) and (B.7) give rise to

$$\phi_{\text{sr1}} < \Delta\phi_{\text{well}} < \phi_{\mathcal{P}_\zeta|_{\text{cl}} > 1} < \phi_0 < \phi_{\text{sr2}}. \quad (\text{B.20})$$

The situation is therefore similar to the case $p > 2$ and $\phi_0 > M_{\text{Pl}}$ described in Sec. B.2.1, and quantum diffusion does not sufficiently suppress PBH production.

B.4 Case $0 < p < 1$

If one takes $p < 1$, contrary to the previous cases, the condition for the classical power spectrum to be larger than one is $\phi > \phi_{\mathcal{P}_\zeta|_{\text{cl}} > 1}$, where $\phi_{\mathcal{P}_\zeta|_{\text{cl}} > 1}$ is given by Eq. (B.7). Furthermore, in this case, the slow-roll conditions read $\phi \gg \phi_{\text{sr}1}$ and $\phi \gg \phi_{\text{sr}2}$, and which of these conditions is the strictest depends on whether ϕ_0 is sub- or super-Planckian.

B.4.1 Case $0 < p < 1$ and $\phi_0 < M_{\text{Pl}}$

In this case the slow-roll condition reads

$$\phi \gg \phi_{\text{sr}1}. \quad (\text{B.21})$$

Since $p < 1$, $\phi_0 < M_{\text{Pl}}$ implies that $\phi_0/M_{\text{Pl}} < v_0^{\frac{p-2}{2p}}$ and from Eqs. (B.2), (B.4) and (B.7), one has

$$\Delta\phi_{\text{well}} < \phi_{\text{sr}1} < \phi_{\mathcal{P}_\zeta|_{\text{cl}} > 1}. \quad (\text{B.22})$$

In this case, stochastic effects cannot play an important role in the slow-roll region of the potential, where the power spectrum is smaller than one provided $\phi < \phi_{\mathcal{P}_\zeta|_{\text{cl}} > 1}$.

B.4.2 Case $0 < p < 1$ and $\phi_0 > M_{\text{Pl}}$

In this case the slow-roll condition reads

$$\phi \gg \phi_{\text{sr}2}, \quad (\text{B.23})$$

and two sub-cases need to be distinguished.

Case $0 < p < 1$ and $\frac{\phi_0}{M_{\text{Pl}}} > v_0^{\frac{p-2}{2p}}$
From Eqs. (B.3), (B.4) and (B.7), one has

$$\phi_{\mathcal{P}_\zeta|_{\text{cl}} > 1} < \phi_{\text{sr}2} < \Delta\phi_{\text{well}}. \quad (\text{B.24})$$

In the classical region of the potential, $\phi > \Delta\phi_{\text{well}}$, the power spectrum is much larger than one and PBHs are overproduced. In the stochastic region of the potential, $\phi_{\text{sr}2} < \phi < \Delta\phi_{\text{well}}$, assuming $\phi_{\text{sr}2} \ll \Delta\phi_{\text{well}}$, μ^2 is given by Eq. (B.5), which is much larger than one for $\phi_0 > M_{\text{Pl}}$ and $p < 2$. Therefore PBHs are also too abundant in this part of the potential, and this case is observationally excluded.

Case $0 < p < 1$ and $1 < \frac{\phi_0}{M_{\text{Pl}}} < v_0^{\frac{p-2}{2p}}$
From Eqs. (B.3), (B.4) and (B.7), one has

$$\Delta\phi_{\text{well}} < \phi_{\text{sr}2} < \phi_{\mathcal{P}_\zeta|_{\text{cl}} > 1}. \quad (\text{B.25})$$

This case is similar to the one where $0 < p < 1$ and $\phi_0 < M_{\text{Pl}}$, and stochastic effects do not play an important role in the slow-roll region of the potential.

B.5 Case $p = 1$

Finally, let us consider the case $p = 1$. The slow-roll approximation is valid throughout the entire vacuum-dominated region of the potential provided

$$\phi_0 \gg M_{\text{Pl}}. \quad (\text{B.26})$$

This case is however more subtle than the previous ones, since from Eq. (5.9), one has

$$\eta_{\text{class}} \equiv 0. \quad (\text{B.27})$$

This means that the first stochastic correction in the classical expansion presented in Sec. 3 vanishes. This does not imply that quantum diffusion never plays a role since higher-order terms can still spoil the classical result, but this suggests that our classicality criterion fails in this case to identify where stochastic effects become important.

This is why no clear conclusion can be drawn in this case. In practice, one should extend the classical expansion of Sec. 3 to next-to-next-to-next to leading order (NNNLO) at least to determine what the first stochastic correction is and under which condition the classical approximation holds, and investigate numerically the cases where it does not. We leave these considerations for future work.

References

- [1] A. A. Starobinsky, *A New Type of Isotropic Cosmological Models Without Singularity*, *Phys. Lett.* **B91** (1980) 99–102.
- [2] K. Sato, *First Order Phase Transition of a Vacuum and Expansion of the Universe*, *Mon.Not.Roy.Astron.Soc.* **195** (1981) 467–479.
- [3] A. H. Guth, *The Inflationary Universe: A Possible Solution to the Horizon and Flatness Problems*, *Phys.Rev.* **D23** (1981) 347–356.
- [4] A. D. Linde, *A New Inflationary Universe Scenario: A Possible Solution of the Horizon, Flatness, Homogeneity, Isotropy and Primordial Monopole Problems*, *Phys.Lett.* **B108** (1982) 389–393.
- [5] A. Albrecht and P. J. Steinhardt, *Cosmology for Grand Unified Theories with Radiatively Induced Symmetry Breaking*, *Phys.Rev.Lett.* **48** (1982) 1220–1223.
- [6] A. D. Linde, *Chaotic Inflation*, *Phys.Lett.* **B129** (1983) 177–181.
- [7] V. F. Mukhanov and G. Chibisov, *Quantum Fluctuation and Nonsingular Universe.*, *JETP Lett.* **33** (1981) 532–535.
- [8] V. F. Mukhanov and G. Chibisov, *The Vacuum energy and large scale structure of the universe*, *Sov.Phys.JETP* **56** (1982) 258–265.
- [9] A. A. Starobinsky, *Dynamics of Phase Transition in the New Inflationary Universe Scenario and Generation of Perturbations*, *Phys.Lett.* **B117** (1982) 175–178.
- [10] A. H. Guth and S. Pi, *Fluctuations in the New Inflationary Universe*, *Phys.Rev.Lett.* **49** (1982) 1110–1113.

- [11] S. Hawking, *The Development of Irregularities in a Single Bubble Inflationary Universe*, *Phys.Lett.* **B115** (1982) 295.
- [12] J. M. Bardeen, P. J. Steinhardt and M. S. Turner, *Spontaneous Creation of Almost Scale - Free Density Perturbations in an Inflationary Universe*, *Phys.Rev.* **D28** (1983) 679.
- [13] PLANCK collaboration, P. A. R. Ade et al., *Planck 2015 results. XIII. Cosmological parameters*, *Astron. Astrophys.* **594** (2016) A13, [[1502.01589](#)].
- [14] PLANCK collaboration, P. Ade et al., *Planck 2015 results. XX. Constraints on inflation*, [1502.02114](#).
- [15] S. Hawking, *Gravitationally collapsed objects of very low mass*, *Mon. Not. Roy. Astron. Soc.* **152** (1971) 75.
- [16] B. J. Carr and S. W. Hawking, *Black holes in the early Universe*, *Mon. Not. Roy. Astron. Soc.* **168** (1974) 399–415.
- [17] B. J. Carr, *The Primordial black hole mass spectrum*, *Astrophys. J.* **201** (1975) 1–19.
- [18] I. Zaballa, A. M. Green, K. A. Malik and M. Sasaki, *Constraints on the primordial curvature perturbation from primordial black holes*, *JCAP* **0703** (2007) 010, [[astro-ph/0612379](#)].
- [19] T. Harada, C.-M. Yoo and K. Kohri, *Threshold of primordial black hole formation*, *Phys. Rev.* **D88** (2013) 084051, [[1309.4201](#)].
- [20] S. Young, C. T. Byrnes and M. Sasaki, *Calculating the mass fraction of primordial black holes*, *JCAP* **1407** (2014) 045, [[1405.7023](#)].
- [21] B. J. Carr, *The primordial black hole mass spectrum*, *ApJ* **201** (Oct., 1975) 1–19.
- [22] M. W. Choptuik, *Universality and scaling in gravitational collapse of a massless scalar field*, *Phys. Rev. Lett.* **70** (1993) 9–12.
- [23] J. C. Niemeyer and K. Jedamzik, *Near-critical gravitational collapse and the initial mass function of primordial black holes*, *Phys. Rev. Lett.* **80** (1998) 5481–5484, [[astro-ph/9709072](#)].
- [24] F. Kuhnel, C. Rampf and M. Sandstad, *Effects of Critical Collapse on Primordial Black-Hole Mass Spectra*, *Eur. Phys. J.* **C76** (2016) 93, [[1512.00488](#)].
- [25] B. J. Carr, K. Kohri, Y. Sendouda and J. Yokoyama, *New cosmological constraints on primordial black holes*, *Phys. Rev.* **D81** (2010) 104019, [[0912.5297](#)].
- [26] B. Carr, M. Raidal, T. Tenkanen, V. Vaskonen and H. Veermae, *Primordial black hole constraints for extended mass functions*, [1705.05567](#).
- [27] V. F. Mukhanov, *Gravitational Instability of the Universe Filled with a Scalar Field*, *JETP Lett.* **41** (1985) 493–496.
- [28] V. F. Mukhanov, *Quantum Theory of Gauge Invariant Cosmological Perturbations*, *Sov. Phys. JETP* **67** (1988) 1297–1302.
- [29] A. A. Starobinsky, *Stochastic de Sitter (inflationary) stage in the early Universe*, *Lect. Notes Phys.* **246** (1986) 107–126.
- [30] Y. Nambu and M. Sasaki, *Stochastic Stage of an Inflationary Universe Model*, *Phys. Lett.* **B205** (1988) 441–446.

- [31] Y. Nambu and M. Sasaki, *Stochastic Approach to Chaotic Inflation and the Distribution of Universes*, *Phys. Lett.* **B219** (1989) 240–246.
- [32] H. E. Kandrup, *Stochastic inflation as a time-dependent random walk*, *Phys. Rev. D* **39** (Apr, 1989) 2245–2252.
- [33] K.-i. Nakao, Y. Nambu and M. Sasaki, *Stochastic Dynamics of New Inflation*, *Prog. Theor. Phys.* **80** (1988) 1041.
- [34] Y. Nambu, *Stochastic Dynamics of an Inflationary Model and Initial Distribution of Universes*, *Prog.Theor.Phys.* **81** (1989) 1037.
- [35] S. Mollerach, S. Matarrese, A. Ortolan and F. Lucchin, *Stochastic inflation in a simple two field model*, *Phys.Rev.* **D44** (1991) 1670–1679.
- [36] A. D. Linde, D. A. Linde and A. Mezhlumian, *From the Big Bang theory to the theory of a stationary universe*, *Phys. Rev.* **D49** (1994) 1783–1826, [[gr-qc/9306035](#)].
- [37] A. A. Starobinsky and J. Yokoyama, *Equilibrium state of a selfinteracting scalar field in the De Sitter background*, *Phys. Rev.* **D50** (1994) 6357–6368, [[astro-ph/9407016](#)].
- [38] A. A. Starobinsky, *Multicomponent de Sitter (Inflationary) Stages and the Generation of Perturbations*, *JETP Lett.* **42** (1985) 152–155.
- [39] M. Sasaki and E. D. Stewart, *A General analytic formula for the spectral index of the density perturbations produced during inflation*, *Prog.Theor.Phys.* **95** (1996) 71–78, [[astro-ph/9507001](#)].
- [40] M. Sasaki and T. Tanaka, *Superhorizon scale dynamics of multiscalar inflation*, *Prog.Theor.Phys.* **99** (1998) 763–782, [[gr-qc/9801017](#)].
- [41] D. H. Lyth, K. A. Malik and M. Sasaki, *A General proof of the conservation of the curvature perturbation*, *JCAP* **0505** (2005) 004, [[astro-ph/0411220](#)].
- [42] D. H. Lyth and Y. Rodriguez, *The Inflationary prediction for primordial non-Gaussianity*, *Phys.Rev.Lett.* **95** (2005) 121302, [[astro-ph/0504045](#)].
- [43] P. Creminelli and M. Zaldarriaga, *Single field consistency relation for the 3-point function*, *JCAP* **0410** (2004) 006, [[astro-ph/0407059](#)].
- [44] D. S. Salopek and J. R. Bond, *Nonlinear evolution of long wavelength metric fluctuations in inflationary models*, *Phys. Rev.* **D42** (1990) 3936–3962.
- [45] E. M. Lifshitz and I. M. Khalatnikov, *About singularities of cosmological solutions of the gravitational equations. I*, *ZhETF* **39** (1960) 149.
- [46] A. A. Starobinsky, *Isotropization of arbitrary cosmological expansion given an effective cosmological constant*, *JETP Lett.* **37** (1983) 66–69.
- [47] G. Comer, N. Deruelle, D. Langlois and J. Parry, *Growth or decay of cosmological inhomogeneities as a function of their equation of state*, *Phys.Rev.* **D49** (1994) 2759–2768.
- [48] I. Khalatnikov, A. Y. Kamenshchik and A. A. Starobinsky, *Comment about quasiisotropic solution of Einstein equations near cosmological singularity*, *Class.Quant.Grav.* **19** (2002) 3845–3850, [[gr-qc/0204045](#)].
- [49] D. Wands, K. A. Malik, D. H. Lyth and A. R. Liddle, *A New approach to the evolution of cosmological perturbations on large scales*, *Phys.Rev.* **D62** (2000) 043527, [[astro-ph/0003278](#)].

- [50] D. H. Lyth and D. Wands, *Conserved cosmological perturbations*, *Phys.Rev.* **D68** (2003) 103515, [[astro-ph/0306498](#)].
- [51] K. Enqvist, S. Nurmi, D. Podolsky and G. Rigopoulos, *On the divergences of inflationary superhorizon perturbations*, *JCAP* **0804** (2008) 025, [[0802.0395](#)].
- [52] T. Fujita, M. Kawasaki, Y. Tada and T. Takesako, *A new algorithm for calculating the curvature perturbations in stochastic inflation*, *JCAP* **1312** (2013) 036, [[1308.4754](#)].
- [53] T. Fujita, M. Kawasaki and Y. Tada, *Non-perturbative approach for curvature perturbations in stochastic- δN formalism*, **1405.2187**.
- [54] V. Vennin and A. A. Starobinsky, *Correlation Functions in Stochastic Inflation*, *Eur. Phys. J.* **C75** (2015) 413, [[1506.04732](#)].
- [55] M. Kawasaki and Y. Tada, *Can massive primordial black holes be produced in mild waterfall hybrid inflation?*, *JCAP* **1608** (2016) 041, [[1512.03515](#)].
- [56] H. Assadullahi, H. Firouzjahi, M. Noorbala, V. Vennin and D. Wands, *Multiple Fields in Stochastic Inflation*, *JCAP* **1606** (2016) 043, [[1604.04502](#)].
- [57] V. Vennin, H. Assadullahi, H. Firouzjahi, M. Noorbala and D. Wands, *Critical Number of Fields in Stochastic Inflation*, **1604.06017**.
- [58] L. Bachelier, *Theorie de la speculation*. Gauthier-Villars, 1900.
- [59] I. Gihman and A. Skorohod, *Stochastic Differential Equations*. Springer Verlag, Berlin Heidelberg New York, 1972, p.108.
- [60] F. W. Olver, D. W. Lozier, R. F. Boisvert and C. W. Clark, *Ch. 13 in NIST Handbook of Mathematical Functions*. Cambridge University Press, New York, NY, USA, 1st ed., 2010.
- [61] M. Abramowitz and I. A. Stegun, *Ch. 13 in Handbook of mathematical functions with formulas, graphs, and mathematical tables*. National Bureau of Standards, Washington, US, ninth ed., 1970.
- [62] F. W. Olver, D. W. Lozier, R. F. Boisvert and C. W. Clark, *Ch. 20 in NIST Handbook of Mathematical Functions*. Cambridge University Press, New York, NY, USA, 1st ed., 2010.
- [63] M. Abramowitz and I. A. Stegun, *Ch. 16 in Handbook of mathematical functions with formulas, graphs, and mathematical tables*. National Bureau of Standards, Washington, US, ninth ed., 1970.
- [64] S. Young and C. T. Byrnes, *Primordial black holes in non-Gaussian regimes*, *JCAP* **1308** (2013) 052, [[1307.4995](#)].
- [65] S. Young, D. Regan and C. T. Byrnes, *Influence of large local and non-local bispectra on primordial black hole abundance*, *JCAP* **1602** (2016) 029, [[1512.07224](#)].
- [66] J. Garcia-Bellido, A. D. Linde and D. Wands, *Density perturbations and black hole formation in hybrid inflation*, *Phys. Rev.* **D54** (1996) 6040–6058, [[astro-ph/9605094](#)].
- [67] A. D. Linde, *Axions in inflationary cosmology*, *Phys. Lett.* **B259** (1991) 38–47.
- [68] A. D. Linde, *Hybrid inflation*, *Phys.Rev.* **D49** (1994) 748–754, [[astro-ph/9307002](#)].
- [69] E. J. Copeland, A. R. Liddle, D. H. Lyth, E. D. Stewart and D. Wands, *False vacuum inflation with Einstein gravity*, *Phys. Rev.* **D49** (1994) 6410–6433, [[astro-ph/9401011](#)].
- [70] S. Renaux-Petel and K. Turzyski, *Geometrical Destabilization of Inflation*, *Phys. Rev. Lett.* **117** (2016) 141301, [[1510.01281](#)].

- [71] S. Renaux-Petel, K. Turzyski and V. Vennin, *Geometrical destabilization, premature end of inflation and Bayesian model selection*, [1706.01835](#).
- [72] E. D. Stewart, *Flattening the inflaton's potential with quantum corrections*, *Phys. Lett.* **B391** (1997) 34–38, [[hep-ph/9606241](#)].
- [73] J. Martin, C. Ringeval and V. Vennin, *Encyclopaedia Inflationaris*, *Phys. Dark Univ.* **5-6** (2014) 75–235, [[1303.3787](#)].
- [74] L. Covi and D. H. Lyth, *Running mass models of inflation, and their observational constraints*, *Phys. Rev.* **D59** (1999) 063515, [[hep-ph/9809562](#)].
- [75] S. M. Leach, I. J. Grivell and A. R. Liddle, *Black hole constraints on the running mass inflation model*, *Phys. Rev.* **D62** (2000) 043516, [[astro-ph/0004296](#)].
- [76] M. Drees and E. Erfani, *Running-Mass Inflation Model and Primordial Black Holes*, *JCAP* **1104** (2011) 005, [[1102.2340](#)].
- [77] Y. Akrami, F. Kuhnel and M. Sandstad, *Uncertainties in primordial black-hole constraints on the primordial power spectrum*, [1611.10069](#).
- [78] F. W. Olver, D. W. Lozier, R. F. Boisvert and C. W. Clark, *Sec. 4.13 in NIST Handbook of Mathematical Functions*. Cambridge University Press, New York, NY, USA, 1st ed., 2010.
- [79] J. Martin, C. Ringeval, R. Trotta and V. Vennin, *The Best Inflationary Models After Planck*, *JCAP* **1403** (2014) 039, [[1312.3529](#)].
- [80] K. Kannike, L. Marzola, M. Raidal and H. Veermäe, *Single Field Double Inflation and Primordial Black Holes*, [1705.06225](#).
- [81] C. Germani and T. Prokopec, *On primordial black holes from an inflection point*, [1706.04226](#).
- [82] H. Motohashi and W. Hu, *Primordial Black Holes and Slow-roll Violation*, [1706.06784](#).
- [83] J. Garcia-Bellido and E. Ruiz Morales, *Primordial black holes from single field models of inflation*, [1702.03901](#).
- [84] J. Grain and V. Vennin, *Stochastic inflation in phase space: Is slow roll a stochastic attractor?*, *JCAP* **1705** (2017) 045, [[1703.00447](#)].
- [85] E. Bugaev and P. Klimai, *Curvature perturbation spectra from waterfall transition, black hole constraints and non-Gaussianity*, *JCAP* **1111** (2011) 028, [[1107.3754](#)].
- [86] E. Bugaev and P. Klimai, *Formation of primordial black holes from non-Gaussian perturbations produced in a waterfall transition*, *Phys. Rev.* **D85** (2012) 103504, [[1112.5601](#)].
- [87] S. Clesse and J. Garcia-Bellido, *Massive Primordial Black Holes from Hybrid Inflation as Dark Matter and the seeds of Galaxies*, *Phys. Rev.* **D92** (2015) 023524, [[1501.07565](#)].
- [88] S. Shandera, A. L. Erickcek, P. Scott and J. Y. Galarza, *Number Counts and Non-Gaussianity*, *Phys. Rev.* **D88** (2013) 103506, [[1211.7361](#)].
- [89] “NIST Digital Library of Mathematical Functions.” <http://dlmf.nist.gov/20.7E30>, Release 1.0.14 of 2016-12-21.
- [90] A. R. Liddle and D. H. Lyth, *Cosmological Inflation and Large-Scale Structure*. Cambridge University Press, 2000, [10.1017/CBO9781139175180](#).